

Event-Driven Receding Horizon Control for Distributed Estimation in Network Systems

Shirantha Welikala and Christos G. Cassandras

Abstract—This paper considers the multi-agent persistent monitoring problem defined on a network (graph) of nodes (targets) with uncertain states. The agent team’s goal is to persistently observe the target states so that an overall measure of estimation error covariance evaluated over a finite period is minimized. Each agent’s trajectory is fully defined by the sequence of targets it visits and the corresponding dwell times spent at each visited target. To find the optimal set of agent trajectories, we propose a distributed and on-line estimation process that requires each agent to solve a sequence of receding horizon control problems (RHCPs) in an event-driven manner. We use a novel objective function form for these RHCPs to optimize the effectiveness of this distributed estimation process and establish its unimodality under certain conditions. Moreover, we show that agents can use machine learning to efficiently solve a significant portion of each RHCP they face without compromising accuracy. Finally, extensive numerical results are provided, indicating significant improvements compared to other agent control methods.

I. INTRODUCTION

We consider the problem of controlling a team of mobile agents equipped with sensing capabilities deployed to monitor a finite set of points of interest (also called *targets*) in a mission space. Each target has stochastic state dynamics and the agent team’s goal is to sense the target states so that an overall target state estimation error metric evaluated over a finite period is minimized. This problem setup is commonly known as the *persistent monitoring* problem and it has many applications such as in surveillance [1], data collection [2], sensing [3] and energy management [4]. In the literature, many variants of this persistent monitoring problem have been studied under different forms of (i) target state dynamic models [5], [6], (ii) global objective functions [7]–[10], (iii) agent dynamic models [11], [12] and (iv) mission spaces [5], [13]–[15].

The work in [5] studies a persistent monitoring problem with deterministic target state dynamics where the agent team aims to minimize the target state values via sensing targets. In this problem setting [5], each target state itself is considered as a measure of uncertainty with no explicit stochasticity and a network (graph) abstraction for this target-agent system is proposed along with a gradient-based solution to find the optimal agent trajectories. The subsequent work in [9] appends a centralized and off-line stage for the solution proposed in [5] that constructs a high performing periodic set of agent trajectories as an initial condition. For the

same persistent monitoring problem, our recent work in [11] develops a distributed and on-line solution based on event-driven receding horizon control (RHC) [16]. This RHC solution has shown to have many attractive features, such as being gradient-free, parameter-free, computationally cheap and adaptive to various forms of state/system perturbations.

In contrast to [5], this paper considers a more challenging persistent monitoring problem, where the target state dynamics are assumed to be stochastic and the agent team is tasked with minimizing the overall *error covariance* associated with target state estimation [7], [17], [18]. In fact, this persistent monitoring problem can also be seen as a distributed estimation problem [19]. Despite the significant differences in the problem setup, the key concepts used in [9] and [11] can still be adopted to address this persistent monitoring problem. Specifically, the work in [7] formulates a minimax problem over an infinite horizon and proposes a periodic, centralized and off-line solution inspired by [9]. As opposed to [7], we use a different objective: the mean overall estimation error covariance evaluated over a finite horizon and develop a distributed and on-line RHC solution inspired by [11].

Similar to [7], the work in [18] considers an infinite horizon objective function and develops a centralized and off-line solution to this persistent monitoring problem. However, compared to [7], [18] uses a different agent measurement model and does not involve graph-based agent trajectory constraints. Nevertheless, both [7] and [18] have been developed focusing only on single-agent cases and thus require additional clustering and assignment stages for deployment in multi-agent scenarios. In contrast, [17] (similar to this work) uses a finite horizon objective function and proposes a distributed solution well-suited for multi-agent cases. However, the solution proposed in [17] is computationally expensive, off-line and time-driven. To address these concerns, this work limits the target state dynamics to a one-dimensional space (as in [5], [9], [11]) and develops a computationally cheap, on-line and event-driven persistent monitoring solution.

In this paper, we first show that each agent’s trajectory is fully defined by the sequence of decisions it makes at specific discrete event times. Next, we formulate a *receding horizon control problem* (RHCP) solved by an agent at any one of these event times. A novel element in this RHCP is that it simultaneously determines the optimal *planning horizon* along with the optimal control decisions, locally at the agent. The determined optimal control decisions are subsequently executed over a shorter *action horizon* defined by the next event that the agent observes, and the same process is continued. Compared to [11], we propose a novel RHCP objective function form that maximizes the utilization

*Supported in part by NSF under grants ECCS-1931600, DMS-1664644, CNS-1645681, by AFOSR under grant FA9550-19-1-0158, by ARPA-E’s NEXTCAR program under grant DE-AR0000796 and by the MathWorks.

The authors are with the Division of Systems Engineering and Center for Information and Systems Engineering, Boston University, Brookline, MA 02446, {shiran27, cgc}@bu.edu.

of the agent sensing capabilities over the planning horizon. Moreover, we study the properties of this RHCP objective function form and establish its unimodality under certain conditions. This ensures that a simple gradient descent algorithm can obtain the globally optimal solution to each RHCP. Next, we show that a machine learning technique can efficiently solve a significant portion of each RHCP that the agents face without compromising the RHCP solution's accuracy. Finally, we investigate how the proposed RHC based agent controllers perform in terms of providing target state estimates and enabling target state controls, compared to other state-of-the-art agent controllers.

This paper is organized as follows. Problem formulation is presented in Section II and a few preliminary theoretical results are discussed in Section III. Section IV and V respectively presents the RHCP formulation and its solution. The subsequent Section VI describes how machine learning can be integrated to solve the RHCPs efficiently. The performance of the proposed RHC method is demonstrated using simulation results in Section VII. Finally, concluding remarks and future work are provided in Section VIII.

II. PROBLEM FORMULATION

We consider M stationary nodes (targets) in the set $\mathcal{V} = \{1, 2, \dots, M\}$ and N mobile agents in the set $\mathcal{A} = \{1, 2, \dots, N\}$. The location of a target $i \in \mathcal{V}$ is fixed at $Y_i \in \mathbb{R}^l$ and the location of an agent $a \in \mathcal{A}$ at time t is denoted by $s_a(t) \in \mathbb{R}^l$ where $l \in \mathbb{Z}_{>0}$ is the dimension of the mission space.

a) Graph Topology: The set of targets \mathcal{V} is assumed to be interconnected according to an undirected graph $\mathcal{G} = (\mathcal{V}, \mathcal{E})$, where $\mathcal{E} \subseteq \{(i, j) : i, j \in \mathcal{V}\}$ represents the set of *trajectory segments* available for agents to travel between targets. Each trajectory segment $(i, j) \in \mathcal{E}$ has an associated value ρ_{ij} that represents the *travel time* between nodes i and j when (i, j) is used by an agent. Trajectory segments are allowed to take arbitrary shapes in \mathbb{R}^l to account for possible constraints in the mission space and in the agent dynamics.

b) Target Dynamics: Each target $i \in \mathcal{V}$ has an associated state $\phi_i(t) \in \mathbb{R}^n$ that follows the dynamics

$$\dot{\phi}_i(t) = A_i \phi_i(t) + B_i v_i(t) + w_i(t), \quad (1)$$

where $\{w_i(t)\}_{i \in \mathcal{V}}$ are mutually independent, zero mean, white, Gaussian distributed processes with $E[w_i(t)w_i'(t)] = Q_i$. In this work, similar to [7], [17], [18], the main focus is on persistently maintaining accurate *target state estimates* exploiting mobile agents as target state sensors. Therefore, in this setting, agents are not responsible for target state control and hence we assume each target i selects (or is aware of) its control input $v_i(t)$.

When an agent visits a target $i \in \mathcal{V}$, it takes the measurements $z_i(t) \in \mathbb{R}^m$ which follows a linear observation model

$$z_i(t) = H_i \phi_i(t) + v_i(t), \quad (2)$$

where $\{v_i(t)\}_{i \in \mathcal{V}}$ are mutually independent, zero mean, white, Gaussian distributed processes with $E[v_i(t)v_i'(t)] = R_i$.

The matrices A_i, B_i, Q_i in (1) and H_i, R_i in (2) are time invariant and known at target $i \in \mathcal{V}$. Moreover, the matrices Q_i and R_i are positive definite.

c) Kalman-Bucy Filter: Considering the models (1), (2), the maximum likelihood estimator $\hat{\phi}_i(t)$ of target state $\phi_i(t)$ is a Kalman-Bucy Filter (evaluated at target i) given by

$$\dot{\hat{\phi}}_i(t) = A_i \hat{\phi}_i(t) + B_i v_i(t) + \eta_i(t) \Omega_i(t) H_i' R_i^{-1} (z_i(t) - H_i \hat{\phi}_i(t)), \quad (3)$$

where $\Omega_i(t)$ is the covariance of the estimation error (i.e., $\Omega_i(t) = E(e_i(t)e_i'(t))$ with $e_i(t) = \phi_i(t) - \hat{\phi}_i(t)$) given by

$$\dot{\Omega}_i(t) = A_i \Omega_i(t) + \Omega_i(t) A_i' + Q_i - \eta_i(t) \Omega_i(t) G_i \Omega_i(t), \quad (4)$$

with $G_i = H_i' R_i^{-1} H_i$ and

$$\eta_i(t) = \mathbf{1}\{\text{Target } i \text{ is observed by an agent at time } t\}, \quad (5)$$

($\mathbf{1}\{\cdot\}$ is the usual indicator function).

According to (4), when a target $i \in \mathcal{V}$ is being observed by an agent (i.e., when $\eta_i(t) = 1$), the covariance $\Omega_i(t)$ decreases and, as a result, the state estimate $\hat{\phi}_i$ becomes more accurate. The opposite occurs when a target is not being observed by an agent. It is also worth pointing out that the dynamics of the covariance $\Omega_i(t)$ (4) are independent of the target state control $v_i(t)$, due to the principle of separation.

d) Agent Model: Based on the adopted graph topology, we assume once an agent $a \in \mathcal{A}$ spends the required travel time to reach a target $i \in \mathcal{V}$, its location $s_a(t)$ falls within a certain range from the target location Y_i that enables establishing a constant sensing ability (i.e., H_i, R_i are fixed) of the target state $\phi_i(t)$. Without loss of generality, we denote the number of agents present at target $i \in \mathcal{V}$ at time t as $N_i(t) = \sum_{a \in \mathcal{A}} \mathbf{1}\{s_a(t) = Y_i\}$.

To simplify the analysis and prevent resource (agent sensing) wastage, similar to [9], [11], we next introduce a control constraint that prevents *simultaneous target sharing* by multiple agents at each target $i \in \mathcal{V}$ as

$$N_i(t) \in \{0, 1\}, \forall t \geq 0. \quad (6)$$

Clearly, this constraint only applies if $N \geq 2$. Moreover, under (6), $\eta_i(t) = N_i(t)$ (see (4)). Also, note that due to the use of a fixed set of travel times $\{\rho_{ij} : (i, j) \in \mathcal{E}\}$, the analysis in this paper is independent of the agent motion dynamic model (similar to the works in [5], [9], [11]). However, with some modifications, the proposed solution can be adapted to accommodate specific agent dynamic models.

e) Global Objective: The goal is to design controllers for the agents to minimize the finite horizon global objective

$$J_T = \frac{1}{T} \int_0^T \sum_{i \in \mathcal{V}} \text{tr}(\Omega_i(t)) dt. \quad (7)$$

The initial condition of this overall persistent monitoring on networks (PMN) problem setup defined by $\phi_i(0)$, $\hat{\phi}_i(0)$ and $\Omega_i(0)$, $\forall i \in \mathcal{V}$, is assumed to be known at respective targets.

f) **Control:** Based on the graph topology \mathcal{G} , we define the *neighbor set* and the *neighborhood* of a target $i \in \mathcal{V}$ as

$$\mathcal{N}_i \triangleq \{j : (i, j) \in \mathcal{E}\} \text{ and } \tilde{\mathcal{N}}_i = \mathcal{N}_i \cup \{i\},$$

respectively. Whenever an agent $a \in \mathcal{A}$ is ready to leave a target $i \in \mathcal{V}$, it selects a *next-visit* target $j \in \mathcal{N}_i$. Thereafter, the agent travels over $(i, j) \in \mathcal{E}$ to arrive at target j after an amount of time ρ_{ij} . Subsequently, it selects a *dwell-time* $u_j \in \mathbb{R}_{\geq 0}$ to spend at target j (which contributes to decreasing $\Omega_j(t)$), and then makes another next-visit decision.

Therefore, the control exerted (by an agent) consists of a sequence of *dwell-times* $u_i \in \mathbb{R}_{\geq 0}$ and *next-visit* targets $j_i \in \mathcal{N}_i$. Our goal is to determine $(u_i(t), j_i(t))$ for any agent residing at a target $i \in \mathcal{V}$ at any time $t \in [0, T]$ which are optimal in the sense of minimizing the global objective (7).

This PMN problem is much more complicated than the well-known NP-Hard traveling salesman problem (TSP) due to: (i) the presence of multiple agents, (ii) the need to determine dwell-times at each visited target, (iii) the target dynamics and (iv) the freedom to make multiple visits to targets. The same reasons make it computationally intractable to apply dynamic programming techniques so as to obtain the optimal controls, even for a relatively simple PMN problem.

g) **Receding Horizon Control:** To address this hard optimization problem, this paper proposes an *Event-Driven Receding Horizon Controller* (RHC) at each agent $a \in \mathcal{A}$. Even though the basic idea of RHC comes from Model Predictive Control (MPC), it exploits the event-driven nature of the considered problem to reduce the complexity by orders of magnitude and provide flexibility in the frequency of control updates. As introduced in [16] and extended later on in [11], [20], [21], the RHC method involves solving an optimization problem of the form (7) limited to a finite *planning horizon*, whenever an event of interest to the controller is observed. The determined optimal controls are then executed over an *action horizon* defined by the occurrence of the next such event. This event-driven process is continued iteratively.

Pertaining to the PMN problem considered in this paper, the RHC, when invoked at time t for an agent residing at target $i \in \mathcal{V}$, aims to determine (i) the immediate dwell-time u_i at target i , (ii) the next-visit target $j \in \mathcal{N}_i$ and (iii) the next dwell-time u_j at target j . Let us denote these controls jointly as $U_i(t) = [u_i(t), j(t), u_j(t)]$. The optimal choice for these controls is obtained by solving an optimization problem of the form

$$U_i^*(t) = \underset{U_i(t) \in \mathbb{U}(t)}{\operatorname{argmin}} [J_H(X_i(t), U_i(t); H) + \hat{J}_H(X_i(t+H))], \quad (8)$$

where $\mathbb{U}(t)$ is the feasible control set at t (exact definition is provided later) and $X_i(t)$ is the current local state. The term $J_H(X_i(t), U_i(t); H)$ represents the immediate cost over the planning horizon $[t, t+H]$ and $\hat{J}_H(X_i(t+H))$ stands for an estimate of the future cost evaluated at $t+H$.

Following the novel *variable horizon* approach proposed in [11], we include the choice of planning horizon H into the optimization problem (8) and ignore the $\hat{J}_H(X_i(t+H))$ term. Due to the scope of this paper, more details on this

modification are omitted here but can be found in [11]. We point out that the proposed RHC method is *distributed* as it allows each agent to separately solve (8) using only local state information.

III. PRELIMINARY RESULTS

According to (4), the error covariance $\Omega_i(t)$ of any target $i \in \mathcal{V}$ is continuous and piece-wise differentiable. Specifically, $\Omega_i(t)$ jumps only when one of the following two (strictly local) *events* occurs: (i) an agent arrival at target i , or (ii) an agent departure from target i . These two events occur alternatively and respectively trigger two different modes of subsequent $\Omega_i(t)$ behaviors, named *active* and *inactive* modes, described by using $\eta_i(t) = 1$ and $\eta_i(t) = 0$ in (4). In the following discussion, we use $\eta_i(t) \in \{0, 1\}$ to represent the mode of target $i \in \mathcal{V}$ and I_n as the identity matrix in \mathbb{R}^n .

Lemma 1: If a target $i \in \mathcal{V}$ is in the mode $\eta_i(t) \in \{0, 1\}$ during a time period $t \in [t_0, t_1]$, its error covariance $\Omega_i(t)$ for any time $t \in [t_0, t_1]$ is given by

$$\Omega_i(t) = C_i(t)D_i^{-1}(t), \text{ where } \begin{bmatrix} C_i(t) \\ D_i(t) \end{bmatrix} = e^{\Psi_i(t-t_0)} \begin{bmatrix} \Omega_i(t_0) \\ I_n \end{bmatrix}, \quad (9)$$

$$\text{and } \Psi_i = \begin{bmatrix} A_i & Q_i \\ \eta_i(t)G_i & -A_i^T \end{bmatrix}.$$

Proof: Omitting the argument t for notational convenience and using the substitution $\Omega_i = C_i D_i^{-1}$ in (4) gives

$$\dot{C}_i - C_i D_i^{-1} \dot{D}_i = (A_i C_i + Q_i D_i) - C_i D_i^{-1} (\eta_i G_i C_i - A_i^T D_i).$$

Equating the coefficients of 1 and $-C_i D_i^{-1}$ terms above gives

$$\begin{bmatrix} \dot{C}_i(t) \\ \dot{D}_i(t) \end{bmatrix} = \begin{bmatrix} A_i & Q_i \\ \eta_i(t)G_i & -A_i^T \end{bmatrix} \begin{bmatrix} C_i(t) \\ D_i(t) \end{bmatrix}.$$

Recall that $\eta_i(t) = 1$ if the target i is active and $\eta_i(t) = 0$ otherwise. Finally, setting the initial conditions: $C_i(t_0) = \Omega_i(t_0)$ and $D_i(t_0) = I_n$, the above linear differential equation can be solved to obtain the result in (9). ■

Using this lemma, a simpler expression for $\Omega_i(t)$ can be derived if the target i is in the inactive mode.

Corollary 1: If a target $i \in \mathcal{V}$ is inactive during $t \in [t_0, t_1]$, the corresponding $\Omega_i(t)$ for any time $t \in [t_0, t_1]$ is given by

$$\begin{aligned} \Omega_i(t) = & \Phi_i(t) \left[\Omega_i(t_0) \right. \\ & \left. + (t-t_0) \int_0^1 (\Phi_i(t))^{-x} Q_i (\Phi_i^T(t))^{-x} dx \right] \Phi_i^T(t), \end{aligned} \quad (10)$$

where $\Phi_i(t) = e^{A_i(t-t_0)}$.

Proof: According to Lemma 1, when $\eta_i(t) = 0$, $\Omega_i(t)$ is given by (9) where Ψ_i is a block triangular matrix. Therefore, $e^{\Psi_i(t-t_0)}$ can be written (using [22, p. 1]) as

$$e^{\Psi_i(t-t_0)} = \begin{bmatrix} \Phi_i(t) & (t-t_0) \int_0^1 (\Phi_i^T(t))^{1-x} Q_i (\Phi_i^T(t))^{-x} dx \\ 0 & (\Phi_i^T(t))^{-1} \end{bmatrix}.$$

Applying this in (9) gives $D_i(t) = \Phi_i^{-1}(t)$ and

$$C_i(t) = \Phi_i(t) \Omega_i(t_0) + (t-t_0) \int_0^1 (\Phi_i^T(t))^{1-x} Q_i (\Phi_i^T(t))^{-x} dx.$$

Finally, $\Omega_i(t) = C_i(t)D_i^{-1}(t)$ yields the $\Omega_i(t)$ expression in Corollary 1. ■

From the above lemma and the corollary, it is clear that the exact form of the $\text{tr}(\Omega_i(t))$ expression required for the global objective (7) cannot be written more compactly - unless the matrices A_i and Ψ_i have some additional properties.

a) **One-Dimensional PMN Problem:** In the remainder of this paper, similar to [5], [9], [11], we constrain ourselves to one-dimensional target state dynamics and agent observation models by setting

$$n = m = 1 \quad (11)$$

in (1) and (2). The goal here is to derive necessary theoretical results to apply the RHC method and then to explore its feasibility for the considered PMN problem. In the long run, we expect to generalize these theoretical results and the RHC solution for multi-dimensional situations. Therefore, we henceforth consider the target parameters A_i, Q_i, H_i, R_i, G_i and the time varying quantities $\phi_i(t), z_i(t), \hat{\phi}_i(t), \Omega_i(t), \forall i \in \mathcal{V}$ as scalars.

b) **Local Contribution:** The contribution to the global objective J_T in (7) by a target $i \in \mathcal{V}$ during a time period $t \in [t_0, t_1]$ is defined as $\frac{1}{T}J_i(t_0, t_1)$ where

$$J_i(t_0, t_1) \triangleq \int_{t_0}^{t_1} \text{tr}(\Omega_i(t))dt = \int_{t_0}^{t_1} \Omega_i(t)dt. \quad (12)$$

We further define the corresponding active and inactive portions of the above local contribution term $J_i(t_0, t_1)$ respectively as $J_i^A(t_0, t_1)$ and $J_i^I(t_0, t_1)$ where

$$\begin{aligned} J_i^A(t_0, t_1) &\triangleq \int_{t_0}^{t_1} \eta_i(t)\Omega_i(t)dt \text{ and} \\ J_i^I(t_0, t_1) &\triangleq \int_{t_0}^{t_1} (1 - \eta_i(t))\Omega_i(t)dt. \end{aligned} \quad (13)$$

Notice that, by definition, $J_i(t_0, t_1) = J_i^A(t_0, t_1) + J_i^I(t_0, t_1)$.

Lemma 2: If a target $i \in \mathcal{V}$ is active during $t \in [t_0, t_1]$, the corresponding $\Omega_i(t)$ for any time $t \in [t_0, t_1]$ is given by

$$\Omega_i(t) = \frac{c_{i1} + c_{i2}e^{-\lambda_i(t-t_0)}}{v_{i1}c_{i1} + v_{i2}c_{i2}e^{-\lambda_i(t-t_0)}}, \quad (14)$$

where $v_{i1}, v_{i2} = \frac{1}{Q_i}(-A_i \pm \sqrt{A_i^2 + Q_i G_i})$, $\lambda_i = 2\sqrt{A_i^2 + Q_i G_i}$, $c_{i1} = v_{i2}\Omega_i(t_0) - 1$ and $c_{i2} = -v_{i1}\Omega_i(t_0) + 1$. The corresponding local contribution $J_i(t_0, t_0 + w)$ in (12) (where $w = (t - t_0)$) is given by $J_i(t_0, t_0 + w) = J_i^A(t_0, t_0 + w)$ where

$$J_i^A(t_0, t_0 + w) = \frac{1}{G_i} \log \left(\frac{v_{i1}c_{i1} + v_{i2}c_{i2}e^{-\lambda_i w}}{v_{i2} - v_{i1}} \right) + \frac{1}{v_{i1}}w. \quad (15)$$

Proof: We first use Lemma 1 to derive (14). Note that $\Psi_i \in \mathbb{R}^{2 \times 2}$ in (9) now can be simplified using $\eta_i(t) = 1$. The eigenvalues of Ψ_i are $\pm \lambda_i/2$ and the corresponding generalized eigenvector matrix is $[1 \ 1; v_{i1} \ v_{i2}]$. Therefore, the matrix exponent $e^{\Psi_i w}$ required in (9) can be evaluated as

$$e^{\Psi_i w} = \begin{bmatrix} 1 & 1 \\ v_{i1} & v_{i2} \end{bmatrix} \begin{bmatrix} e^{\frac{\lambda_i w}{2}} & 0 \\ 0 & e^{-\frac{\lambda_i w}{2}} \end{bmatrix} \begin{bmatrix} 1 & 1 \\ v_{i1} & v_{i2} \end{bmatrix}^{-1}.$$

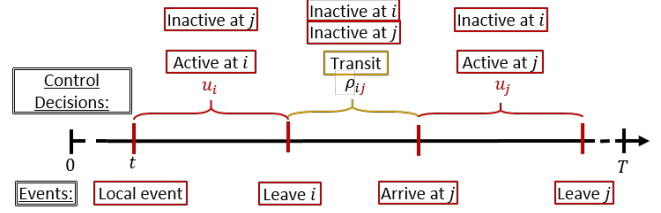


Fig. 1: Event timeline and control decisions under RHC.

Applying this result in (9) gives

$$\begin{bmatrix} C_i(t) \\ D_i(t) \end{bmatrix} = e^{\frac{\lambda_i w}{2}} \begin{bmatrix} v_{i2} - v_{i1}e^{-\lambda_i w} & -1 + e^{-\lambda_i w} \\ v_{i1}v_{i2}(1 - e^{-\lambda_i w}) & -v_{i1} + v_{i2}e^{\lambda_i w} \end{bmatrix} \begin{bmatrix} \Omega_i(t_0) \\ 1 \end{bmatrix}.$$

Since $\Omega_i(t) = C_i(t)/D_i(t)$ (from (9)), we now can use the above result to obtain (14).

Finally, based on (13), the relationship in (15) can be obtained by analytically evaluating the integral of $\Omega_i(t)$:

$$J_i^A(t_0, t_0 + w) = \int_{t_0}^{t_0+w} \frac{c_{i1} + c_{i2}e^{-\lambda_i(\tau-t_0)}}{v_{i1}c_{i1} + v_{i2}c_{i2}e^{-\lambda_i(\tau-t_0)}} d\tau. \quad \blacksquare$$

Lemma 3: If a target $i \in \mathcal{V}$ is inactive during $t \in [t_0, t_1]$, the corresponding $\Omega_i(t)$ for any time $t \in [t_0, t_1]$ is given by

$$\Omega_i(t) = \left(\Omega_i(t_0) + \frac{Q_i}{2A_i} \right) e^{2A_i(t-t_0)} - \frac{Q_i}{2A_i}. \quad (16)$$

The corresponding local contribution $J_i(t_0, t_0 + w)$ (where $w = (t - t_0)$) is given by $J_i(t_0, t_0 + w) = J_i^I(t_0, t_0 + w)$ where

$$J_i^I(t_0, t_0 + w) = \frac{1}{2A_i} \left(\Omega_i(t_0) + \frac{Q_i}{2A_i} \right) (e^{2A_i w} - 1) - \frac{Q_i}{2A_i}w. \quad (17)$$

Proof: These two results (16) and (17) can be proved by using Ψ_i in (9) as $\Psi_i = [A_i \ Q_i; 0 \ -A_i^T]$ and following the same steps used in the proof of Lemma 2. ■

IV. RHC PROBLEM (RHCP) FORMULATION

Let us consider a situation where an agent $a \in \mathcal{A}$ resides at a target $i \in \mathcal{V}$ at some time $t \in [0, T]$. Due to the distributed setting, note that we assume agent a is made aware of only *local events* occurring in the neighborhood \mathcal{N}_i (similar to [11]). As mentioned earlier, the control $U_i(t)$ in (8) consists of the dwell-time u_i at the current target i , the next-visit target $j \in \mathcal{N}_i$, and the dwell-time u_j at the next-visit target j (see Fig. 1). Therefore, agent a has to optimally select three decision variables (control vector): $U_i(t) \triangleq [u_i(t), j(t), u_j(t)]$.

a) **Planning Horizon:** Based on (8), notice that the RHC depends on the planning horizon $H \in \mathbb{R}_{\geq 0}$ which here is viewed as a *fixed* control parameter. Moreover, since $t + H$ in (8) is constrained by $t + H \leq T$, if this is violated, we truncate the planning horizon to be $H = T - t$.

b) **The RHCP:** Let us decompose the control $U_i(t)$ into its real-valued components $U_{ij} \triangleq [u_i, u_j]$ and its discrete component j (omitting time arguments). The current local state is taken as $X_i(t) = \{\Omega_j(t) : j \in \mathcal{N}_i\}$. Then, the optimal controls

are obtained by solving the following set of optimization problems, henceforth called the RHC Problem (RHCP):

$$U_{ij}^* = \arg \min_{U_{ij} \in \mathbb{U}} J_H(X_i(t), U_{ij}; H); \quad \forall j \in \mathcal{N}_i, \text{ and,} \quad (18)$$

$$j^* = \arg \min_{j \in \mathcal{N}_i} J_H(X_i(t), U_{ij}^*; H). \quad (19)$$

Before getting into details, note that (18) involves solving $|\mathcal{N}_i|$ of optimization problems, one for each neighbor $j \in \mathcal{N}_i$ ($|\cdot|$ denotes the cardinality operator or the 1-norm depending on the argument). Then, (19) determines j^* through a simple numerical comparison. Therefore, the final optimal control decision $U_i^*(t)$ of (8) is the composition: $U_i^*(t) = \{U_{ij^*}^*, j^*\}$.

The RHCP objective function $J_H(\cdot)$ is chosen in terms of the *local objective* function of target i , which is denoted by $\bar{J}_i(t_0, t_1)$ over any interval $[t_0, t_1] \subseteq [0, T]$. The exact definition of $\bar{J}_i(t_0, t_1)$ is provided later on (see (22)).

c) **Variable Horizon:** In a conventional RHC setting, a RHC objective function is evaluated over a fixed planning horizon (e.g., $[t, t+H] \subseteq [0, T]$, where H is predefined). This leads to control solutions that are dependent on the choice of planning horizon H . When developing on-line control methods, having such a dependence on a predefined parameter is unfavorable, as now the controller does not have the opportunity to fine-tune H and re-evaluate its controls.

In this paper, the proposed RHC is made free of the planning horizon parameter value H by adopting the concept of *variable horizon* proposed in [11]. First, we redefine the planning horizon as w (instead of H) where we set

$$w = w(U_i) \triangleq |U_{ij}| + \rho_{ij} = u_i + \rho_{ij} + u_j. \quad (20)$$

Note that $w = w(U_i)$ is now a control dependent variable that covers exclusively the horizon over which the RHCP is solved (see Fig. 1). Next, we use the predefined parameter H to constrain w through $w(U_i) = u_i + \rho_{ij} + u_j \leq H$. Finally, we define the RHCP objective function as the local objective function of target i evaluated over the planning horizon: $[t, t+w]$. In a nutshell, the objective function J_H and the feasible control space \mathbb{U} of the RHCP ((18) and (19)) are chosen as

$$J_H(X_i(t), U_{ij}; H) = \bar{J}_i(t, t+w) \quad \text{and} \quad (21)$$

$$\mathbb{U} = \{U : U \in \mathbb{R}^2, U \geq 0, |U| + \rho_{ij} \leq H\}.$$

As pointed out in [11], this modification makes the RHCP solution free of the parameter H as long as it is sufficiently large. Moreover, this RHCP formulation simultaneously determines the optimal planning horizon size $w^* = |U_{ij^*}^*| + \rho_{ij^*}$ in terms of the optimal control $U_i^*(t) = \{U_{ij^*}^*, j^*\}$.

d) **Local Objective:** We denote the *local objective function* of a target $i \in \mathcal{V}$ over a period $[t_0, t_1] \subseteq [0, T]$ as $\bar{J}_i(t_0, t_1)$. The purpose of \bar{J}_i is to be used in (21) as the RHCP objective by each agent (visiting target i) for the selection of its controls $U_i = [u_i, j, u_j]$. The functions J_i and $\sum_{j \in \mathcal{N}_i} J_j$ are two conventional candidates for \bar{J}_i [11]. However, note that: (i) \bar{J}_i needs to be evaluated over $[t, t+w]$ in (21) where $w = u_i + \rho_{ij} + u_j$ (20), (ii) The candidates J_i and $\sum_{j \in \mathcal{N}_i} J_j$ can be written as summations of the contribution terms in (15),(17) and (iii) it is easy to see that both (15),(17) increase

monotonically with w . As a result, when minimizing \bar{J}_i , both candidate forms of \bar{J}_i yield the controls $u_i^* = 0, u_j^* = 0$ in an attempt to minimize $w = w(U_i)$ (making $w^* = \rho_{ij}$). This would imply that no agent ever dwells at any target.

Therefore, we propose an alternative local objective:

$$\bar{J}_i(t_0, t_1) \triangleq - \frac{\sum_{j \in \mathcal{N}_i} \bar{J}_j^A(t_0, t_1)}{\sum_{j \in \mathcal{N}_i} J_j(t_0, t_1)}. \quad (22)$$

which represents the *normalized active contribution* (i.e., the contribution during agent visits in (13)) of the targets in the neighborhood \mathcal{N}_i over the interval $[t_0, t_1]$. As a result of this form, when it is used as the RHCP objective function (21), the agent (residing at target i) will have to optimally allocate its sensing capabilities (resources) over the target i and the next-visit target $j \in \mathcal{N}_i$ (i.e., have to optimally select the controls u_i and u_j). Moreover, we will show that this local objective function is unimodal in most cases of interest.

To highlight the relationship between the local objective (22) and the global objective (7), let us define the global version of (22), by setting $t_0 = 0, t_1 = T, \mathcal{N}_i = \mathcal{V}$ in (22) as

$$\hat{J}_T \triangleq - \frac{\sum_{i \in \mathcal{V}} J_i^A(0, T)}{\sum_{i \in \mathcal{V}} J_i(0, T)}. \quad (23)$$

Notice that the denominator of \hat{J}_T is proportional to the global objective J_T in (7) as $J_T = \frac{1}{T} \sum_{i \in \mathcal{V}} J_i(0, T)$. Moreover, the numerator of \hat{J}_T measures how effectively agents allocate their sensing resources over the network over the period $[0, T]$. Therefore, we can conclude that agents minimizing a local version of (23) (i.e., (22)) can in fact lead to minimizing (7) (notice the negative sign in (22)).

Further, numerical experiments show that both J_t and \hat{J}_t profiles under the same agent controls for $t \in [0, T]$ behave in the same manner after a brief transient phase (e.g., see Fig 2(a)). Furthermore, when the instantaneous values of J_t and \hat{J}_t (i.e., evaluated over a very small period $[t, t+\Delta]$) are compared for $t \in [0, T-\Delta]$, we observe that \hat{J}_t is more sensitive to the variations of the system (while remaining within a small interval) compared to J_t (e.g., see Fig 2(b)). These qualities imply the feasibility of (22) as the local objective function for the use of agents to decide their controls so as to optimize the global objective (7).

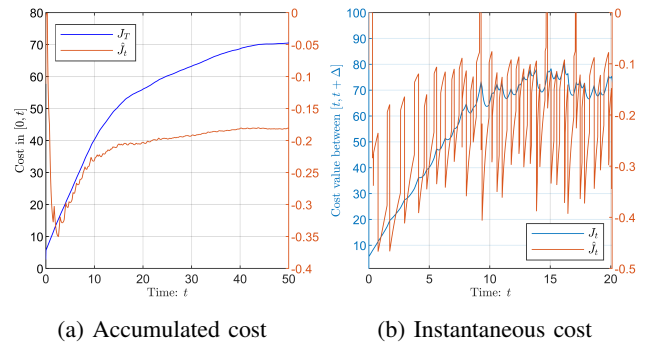


Fig. 2: Comparison between J_t in (7) and \hat{J}_t in (23)

To evaluate the local objective function $\bar{J}_i(t_0, t_1)$ in (22), first, $J_j^A(t_0, t_1)$ terms are evaluated using Lemma 2. Next,

corresponding $J_j^I(t_0, t_1)$ terms are evaluated using Corollary 3. Finally, these two results are combined to obtain the necessary $J_j(t_0, t_1)$ terms for (22).

e) **Event-Driven Action Horizon:** Similar to all receding horizon controllers, an optimal receding horizon control solution computed over a certain planning horizon is executed only over a shorter *action horizon*. In this event-driven persistent monitoring setting, the value of h is determined by the first event that takes place after the time t (when the RHCP was last solved). Therefore, in the proposed RHC approach, the control is updated whenever asynchronous events occur. Thus, it prevents unnecessary steps to re-solve the RHCP (i.e., (18)-(19) with (21)) unlike time-driven receding horizon control.

In general, the determination of the action horizon h may be controllable or uncontrolled. The latter case occurs as a result of random or external events in the system (if such events are part of the setting), while the former corresponds to the occurrence of any one event resulting from an agent finishing the execution of a RHCP solution determined at an earlier time. Next, we define two *controllable* events associated with an agent when it resides at target i . Both of these events define the action horizon h based on the RHCP solution $U_i^*(t)$ obtained by the agent at time $t \in [0, T]$:

1. Event $[h \rightarrow u_i^*]$: This event occurs at time $t + u_i^*(t)$ and indicates the termination of the active time at target i . By definition, this coincides with a departure event from i .

2. Event $[h \rightarrow \rho_{ij}^*]$: This event occurs at time $t + \rho_{ij}^*$ and is only feasible after an event $[h \rightarrow u_i^*]$ has occurred (including the possibility that $u_i^*(t) = 0$). Clearly, this coincides with an arrival event at target j^* .

Among these two types of events, only one is feasible at any one time. However, it is also possible for a different event to occur after t , before one of these two events occurs. Such an event is either external, random (if our model allows for such events) or is controllable but associated with a different target than i . In particular, let us define two additional events that may occur at any neighbor $j \in \mathcal{N}_i$ and affect the agent residing at i . These events aim to ensure the control constraint (6) and apply only to multi-agent persistent monitoring problems.

At time t , if a target $j \in \mathcal{V}$ already has a residing agent or if an agent is en route to visit it from a neighboring target in \mathcal{N}_j , it is said to be *covered*. Now, an agent $a \in \mathcal{A}$ residing at target i can prevent target sharing at $j \in \mathcal{N}_i$ by simply modifying the neighbor set \mathcal{N}_i used in its RHCP solved at time t to exclude all such covered targets. Let us use $\mathcal{N}_i(t)$ to indicate a *time-varying* neighborhood of i . Then, if target j becomes covered at t , we set $\mathcal{N}_i(t) = \mathcal{N}_i(t^-) \setminus \{j\}$. Most importantly, note that as soon as an agent a is en route to j^* , j^* becomes covered, thus preventing any other agent from visiting j^* prior to agent a 's subsequent departure from j^* .

Based on this discussion, we define the following two additional *neighbor-induced local events* at $j \in \mathcal{N}_i$ affecting an agent a residing at target i :

3. Covering Event C_j , $j \in \mathcal{N}_i$: This event causes $\mathcal{N}_i(t)$ to be modified to $\mathcal{N}_i(t) \setminus \{j\}$.

4. Uncovering Event \bar{C}_j , $j \in \mathcal{N}_i$: This event causes $\mathcal{N}_i(t)$ to be modified to $\mathcal{N}_i(t) \cup \{j\}$.

If one of these two events takes place while an agent remains active at target i (prior to an occurrence of event $[h \rightarrow u_i^*]$), then the RHCP is re-solved to account for the updated $\mathcal{N}_i(t)$. This may affect the optimal solution's values U_i^* compared to the previous solution. Note, however, that the new solution will still give rise to a subsequent event $[h \rightarrow u_i^*]$.

f) **Two Forms of RHCPs:** Note that the exact form of the RHCP to be solved at time t depends on the event that triggered the end of the previous action horizon. In particular, there are two possible forms of RHCPs as follows.

1. RHCP1: This problem is solved by an agent when an event $[h \rightarrow \rho_{ki}]$ occurs at time t at target i for any $k \in \mathcal{N}_i(t)$, i.e., at the arrival of the agent at target i . The solution $U_i^*(t)$ includes $u_i^*(t) \geq 0$, representing active time to be spent at i . This problem may also be solved while the agent is active at i if a C_j or \bar{C}_j event occurs at any neighbor $j \in \mathcal{N}_i(t)$.

2. RHCP2: This problem is solved by an agent residing at target i when an event $[h \rightarrow u_i^*]$ occurs at time t . The solution $U_i^*(t)$ is now constrained to include $u_i^*(t) = 0$ by default, implying that the agent must immediately depart from i .

V. SOLVING THE EVENT-DRIVEN RECEDING HORIZON CONTROL PROBLEMS

This section presents the solutions to the identified two forms of RHCPs. We begin with **RHCP2** because it is the simplest problem given that in this case $u_i^*(t) = 0$ by default and U_{ij} in (18) is limited to $U_{ij} = [u_j]$.

A. Solution of the RHCP2

In this case, the variable horizon w in (20) becomes $w = \rho_{ij} + u_j$. Based on the control constraints (21): $w = \rho_{ij} + u_j \leq H$ and $u_j \geq 0$, any target $j \in \mathcal{N}_i(t)$ such that $\rho_{ij} > H$ will not result in a feasible dwell-time value u_j . Therefore, such targets are directly omitted from (18).

a) **Constraints:** In this RHCP, u_j is constrained as:

$$0 \leq u_j \leq H - \rho_{ij}. \quad (24)$$

b) **Objective:** Following (21), the objective function for **RHCP2** is $\bar{J}_i(t, t+w)$. To obtain an exact expression for \bar{J}_i , it is decomposed using (22) as

$$\bar{J}_i = -\frac{J_j^A + \sum_{k \in \mathcal{N}_i(t) \setminus \{j\}} J_k^A}{(J_j^A + J_j^I) + \sum_{k \in \mathcal{N}_i(t) \setminus \{j\}} (J_k^A + J_k^I)} = -\frac{J_j^A}{J_j^A + J_j^I + \sum_{k \in \mathcal{N}_i(t) \setminus \{j\}} J_k^I}. \quad (25)$$

Notice that each term in (25) is evaluated over the planning horizon $[t, t+w]$. Therefore $J_k^A = J_k^A(t, t+w) = 0$ as any target $k \in \mathcal{N}_i \setminus \{j\}$ is not being visited during the planning horizon

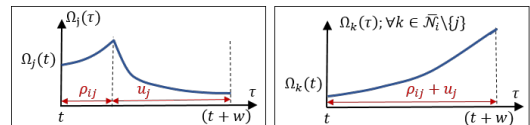


Fig. 3: State trajectories during $[t, t+w]$ for **RHCP2**.

(see Fig. 3). Similarly, using Fig. 3, we can write $J_j^A = J_j(t + \rho_{ij}, t + \rho_{ij} + u_j)$, $J_j^I = J_j(t, t + \rho_{ij})$ and $J_k^I = J_k(t, t + \rho_{ij} + u_j)$. Each of these terms can be evaluated using Lemmas 2 and 3. These results together with (25) give the objective function $\bar{J}_i(t, t + w)$ required for **RHCP2** in the form $\bar{J}_i(u_j)$ (with a slight abuse of notation) where

$$\bar{J}_i(u_j) = -\frac{A(u_j)}{A(u_j) + B(u_j)}, \quad (26)$$

where we define

$$A(u_j) \triangleq J_j^A = c_1 + c_2 \log(1 + c_3 e^{-\lambda_j u_j}) + c_4 u_j, \quad (27)$$

$$B(u_j) \triangleq J_j^I + \sum_k J_k^I = c_5 + c_6 u_j + \sum_k c_{7k} e^{2A_k u_j}, \quad (28)$$

with $\lambda_j = 2\sqrt{A_j^2 + Q_j G_j}$ and

$$\begin{aligned} c_1 &= -c_2 \log(1 + c_3), \quad c_2 = \frac{1}{G_j}, \quad c_3 = -\frac{G_j \Omega_j' + Q_j v_{j2}}{G_j \Omega_j' + Q_j v_{j1}}, \\ \Omega_j' &= \Omega_j(t + \rho_{ij}), \quad v_{j1}, v_{j2} = \frac{1}{Q_j} (-A_j \pm \sqrt{A_j^2 + Q_j G_j}), \\ c_4 &= \frac{1}{v_{j1}}, \quad c_5 = \frac{1}{2A_j} \left(\Omega_j + \frac{Q_j}{2A_j} \right) \times (e^{2A_j \rho_{ij}} - 1) - \frac{Q_j \rho_{ij}}{2A_j} \\ &\quad - \sum_k \frac{1}{2A_k} \left(\Omega_k + \frac{Q_k}{2A_k} + Q_k \rho_{ij} \right), \quad \Omega_j = \Omega_j(t), \\ \Omega_k &= \Omega_k(t), \quad c_6 = -\sum_k \frac{Q_k}{2A_k}, \quad c_{7k} = \frac{1}{2A_k} \left(\Omega_k + \frac{Q_k}{2A_k} \right) e^{2A_k \rho_{ij}}. \end{aligned} \quad (29)$$

c) **Unimodality of $\bar{J}_i(u_j)$** : To establish the unimodality of $\bar{J}_i(u_j)$, we first prove the following lemma.

Lemma 4: The **RHCP2** objective function $\bar{J}_i(u_j)$ (26) satisfies the following limits:

$$\lim_{u_j \rightarrow 0} \bar{J}_i(u_j) = 0 \quad \text{and} \quad (30)$$

$$\lim_{u_j \rightarrow \infty} \bar{J}_i(u_j) = \begin{cases} L_i & \text{if } A_k < 0, \forall k \in \mathcal{N}_i \setminus \{j\}, \\ 0 & \text{otherwise,} \end{cases} \quad (31)$$

where $L_i = -1/(1 + \frac{c_6}{c_4})$ (c_4, c_6 are defined in (29)) and all limits are approached from below.

Proof: To establish these two results, we exploit the $A(u_j), B(u_j)$ notation introduced in (26). The result in (30) is proved using the relationships: $\lim_{u_j \rightarrow 0} A(u_j) = 0$ (note that, from (29): $c_1 + c_2 \log(1 + c_3) = 0$) and $\lim_{u_j \rightarrow 0^+} B(u_j) = c_5 + \sum_k c_{7k} \geq 0$. Similarly, (31) is proved using the limit (given by L'Hospital's rule):

$$\lim_{u_j \rightarrow \infty} \frac{B(u_j)}{A(u_j)} = \begin{cases} \frac{c_6}{c_4} & \text{if } A_k < 0, \forall k \in \mathcal{N}_i \setminus \{j\}, \\ \infty & \text{otherwise.} \end{cases} \quad \blacksquare$$

We next make the following assumption related to the neighborhood $\mathcal{N}_i \setminus \{j\}$ of target i , regarding the neighboring target states $\Omega_k(t)$ and parameters A_k, Q_k for all $k \in \mathcal{N}_i \setminus \{j\}$.

Assumption 1: $\sum_{k \in \mathcal{N}_i \setminus \{j\}} (2\Omega_k(t)A_k + Q_k) > 0$.

Since $\Omega_k(t) > 0, \forall k, t$ and $Q_k > 0, \forall k$, Assumption 1 holds whenever $A_k \geq 0, \forall k$ (i.e., whenever the target dynamics (1) are unstable). We point out that assuming $A_k \geq 0, \forall k$ is also used in [7] and in fact it makes the target state estimation

problem more challenging. In the case where $A_k < 0$, based on Lemma 3 (assuming no agent visits at target k), $\Omega_k(t)$ will asymptotically converge to $-Q_k/(2A_k)$ from its initial value $\Omega_k(0)$. Therefore, whenever such a stable target k satisfies $\Omega_k(0) > -Q_k/(2A_k)$, it will still not affect Assumption 1 as $(2\Omega_k(t)A_k + Q_k) > 0, \forall t$. In short, this assumption is a mild one (it just requires a bound on the initial covariance).

Note that according to Lemma 2, if a target $i \in \mathcal{V}$ is sensed by an agent for an infinite duration of time, its error covariance $\Omega_i(t)$ will converge to the steady state value $\Omega_{i,ss}$:

$$\Omega_{i,ss} = \lim_{t \rightarrow \infty} \Omega_i(t) = \frac{1}{v_{i1}} = \frac{Q_i}{-A_i + \sqrt{A_i^2 + Q_i G_i}}. \quad (32)$$

This $\Omega_{i,ss}$ value is a characteristic of target i . It also represents the minimum achievable error covariance level at target i . Therefore, in practice, we can expect $\Omega_i(0) \geq \Omega_{i,ss}$ which will also imply (using (4)):

$$\Omega_i(t) > \Omega_{i,ss}, \quad \forall i \in \mathcal{V}, \quad \forall t \in [0, T]. \quad (33)$$

Even if $\Omega_i(0) < \Omega_{i,ss}$, $\Omega_i(t)$ will increase beyond $\Omega_{i,ss}$ value (with or without agent sensing) and henceforth the condition in (33) will hold.

Each target $i \in \mathcal{V}$ with $A_i < 0$ (i.e., stable) will have its covariance value $\Omega_i(t)$ bounded inside the interval $(\Omega_{i,ss}, \bar{\Omega}_{i,ss})$ where $\bar{\Omega}_{i,ss} = -Q_i/(2A_i)$, after an initial travel phase. In other words, $(\Omega_{i,ss}, \bar{\Omega}_{i,ss})$ is a globally attractive positively invariant set for (4). For targets with $A_k \geq 0$, this invariant set is $(\Omega_{i,ss}, \infty)$.

Theorem 1: Under Assumption 1, the objective function of **RHCP2** in (26) is unimodal.

Proof: Again we exploit the $A(u_j), B(u_j)$ notation introduced in (26). Seeing $A(u_j)$ and $B(u_j)$ (defined respectively in (27) and (28)) as contributions of the targets, it is clear that $A(u_j) \geq 0$ and $B(u_j) \geq 0$ for all $u_j \in \mathbb{R}_{\geq 0}$. Therefore, based on (26), $\bar{J}_i(u_j) \leq 0$ for all $u_j \in \mathbb{R}_{\geq 0}$. Now, according to the limits of $\bar{J}_i(u_j)$ established in Lemma 4, it is clear that $\bar{J}_i(u_j)$ has at least one or more local minimizers.

Through differentiating (26), we can obtain an equation for the stationary points of $\bar{J}_i(u_j)$ as:

$$\frac{d\bar{J}_i(u_j)}{du_j} = 0 \iff A(u_j) \frac{dB(u_j)}{du_j} - B(u_j) \frac{dA(u_j)}{du_j} = 0.$$

For notational convenience, let us re-write the above equation as $AB' - BA' = 0$. Using the same notation, the second derivative of $\bar{J}_i(u_j)$ can be written as

$$\frac{d^2 \bar{J}_i(u_j)}{du_j^2} = \frac{AB'' - BA''}{(A+B)^2} - \frac{(AB' - BA')(A' + B')}{(A+B)^3}.$$

Therefore, the nature of a stationary point of $\bar{J}_i(u_j)$ is determined by the sign of the term $AB'' - BA''$. Since we already know $A, B \geq 0$, let us focus on the A'' and B'' terms.

Using the $A(u_j)$ expression (i.e., (27)) we can write

$$A'' = \frac{d^2 A(u_j)}{du_j^2} = \frac{c_3 c_2 \lambda_j^2 e^{-\lambda_j u_j}}{(c_3 + e^{-\lambda_j u_j})^2}. \quad (34)$$

From (29), clearly, $c_2 > 0$ and

$$\begin{aligned} c_3 < 0 &\iff \Omega_j(t + \rho_{ij}) > -\frac{Q_j v_{j2}}{G_j} \\ &= \frac{1}{v_{j1}} \\ &= \Omega_{j,ss}. \end{aligned}$$

The last two steps respectively used the relationships $v_{j1}v_{j2} = -\frac{G_j}{Q_j}$ and (32). Since $\Omega_j(t + \rho_{ij}) > \Omega_{j,ss}$ (see (33)), $c_3 < 0$ and thus (34) implies that $A'' < 0, \forall u_j \geq 0$.

Using the $B(u_j)$ expression (i.e., (28)), we can write

$$B'' = \frac{d^2 B(u_j)}{du_j^2} = \sum_{k \in \mathcal{N}_i \setminus \{j\}} (2\Omega_k(t)A_k + Q_k) e^{2A_k(\rho_{ij} + u_j)}. \quad (35)$$

Notice that the Assumption 1 is satisfied if and only if:

$$\begin{aligned} &\sum_{\substack{k:A_k \geq 0, \\ k \in \mathcal{N}_i \setminus \{j\}}} (2\Omega_k(t)A_k + Q_k) > - \sum_{\substack{k:A_k < 0, \\ k \in \mathcal{N}_i \setminus \{j\}}} (2\Omega_k(t)A_k + Q_k) \\ \implies &\sum_{\substack{k:A_k \geq 0, \\ k \in \mathcal{N}_i \setminus \{j\}}} (2\Omega_k(t)A_k + Q_k) e^{2A_k(\rho_{ij} + u_j)} \\ &> - \sum_{\substack{k:A_k < 0, \\ k \in \mathcal{N}_i \setminus \{j\}}} (2\Omega_k(t)A_k + Q_k) e^{2A_k(\rho_{ij} + u_j)} \\ \implies &\sum_{k \in \mathcal{N}_i \setminus \{j\}} (2\Omega_k(t)A_k + Q_k) e^{2A_k(\rho_{ij} + u_j)} > 0. \end{aligned}$$

The second step above is a result of the monotonicity of the exponential function. This final result and (35) implies that $B'' > 0, \forall u_j \geq 0$.

We have shown that $A, B, B'' > 0$ while $A'' < 0, \forall u_j \geq 0$. Therefore, $AB'' - BA'' > 0, \forall u_j \geq 0$. Thus, all the stationary points of $\bar{J}_i(u_j)$ should be local minimizers. Since $\bar{J}_i(u_j)$ and all its derivatives are continuous, it cannot have two (or more) local minimizers without having a local maximizer(s). Therefore, $\bar{J}_i(u_j)$ has only one stationary point which is the global minimizer and thus $\bar{J}_i(u_j)$ is unimodal. ■

d) **Solving RHCP2 for optimal control u_j^*** : The solution u_j^* of (18) is given by

$$u_j^* = \arg \min_{0 \leq u_j \leq H - \rho_{ij}} \bar{J}_i(u_j). \quad (36)$$

Since the objective function is unimodal and the feasible space is convex, we use the projected gradient descent algorithm to obtain the globally optimal control decision u_j^* .

e) **Solving for Optimal Next-Visit Target j^*** : Using the obtained u_j^* values in (36) for all $j \in \mathcal{N}_i(t)$, we now know the optimal trajectory costs $\bar{J}_i(u_j^*), \forall j \in \mathcal{N}_i(t)$. Based on (19), the optimal target to visit next is

$$j^* = \arg \min_{j \in \mathcal{N}_i(t)} \bar{J}_i(u_j^*). \quad (37)$$

Thus, upon solving **RHCP2**, agent a departs from target i at time t and follows the path $(i, j^*) \in \mathcal{E}$ to visit target j^* . In the spirit of RHC, recall that the optimal control will be updated upon the occurrence of the next event, which, in this case, will be the arrival of the agent at j^* , triggering the solution of an instance of **RHCP1** at target j^* .

B. Solution of RHCP1

We next consider the **RHCP1**, which is the most general version among the two RHCP forms. In **RHCP1**, U_{ij} in (18) is directly $U_{ij} = [u_i, u_j]$ and the variable horizon w is the same as in (20), where $w = u_i + \rho_{ij} + u_j$.

a) **Constraints**: In this RHCP setup u_i and u_j are constrained as:

$$0 \leq u_i, \quad 0 \leq u_j, \quad u_i + u_j \leq H - \rho_{ij}. \quad (38)$$

b) **Objective**: Following (21), the objective function for **RHCP1** is $\bar{J}_i(t, t+w)$. To obtain an exact expression for \bar{J}_i , it is decomposed using (22) as

$$\begin{aligned} \bar{J}_i &= -\frac{J_i^A + J_j^A + \sum_{k \in \mathcal{N}_i(t) \setminus \{j\}} J_k^A}{(J_i^A + J_i^J) + (J_j^A + J_j^J) + \sum_{k \in \mathcal{N}_i(t) \setminus \{j\}} (J_k^A + J_k^J)} \\ &= -\frac{J_i^A + J_j^A}{(J_i^A + J_j^A) + (J_i^J + J_j^J) + \sum_{k \in \mathcal{N}_i(t) \setminus \{j\}} J_k^J}. \end{aligned} \quad (39)$$

Similar to (25), note that each term in (39) is also evaluated over the planning horizon $[t, t+w]$. Therefore $J_k^A = J_k^A(t, t+w) = 0$ as any target $k \in \mathcal{N}_i \setminus \{j\}$ is not being visited during the planning horizon (see Fig. 4). Moreover, using Fig. 4 we can write $J_i^A = J_i(t, t+u_i)$, $J_j^A = J_j(t+u_i + \rho_{ij}, t+u_i + \rho_{ij} + u_j)$, $J_i^J = J_i(t+u_i, t+u_i + \rho_{ij} + u_j)$, $J_j^J = J_j(t, t+u_i + \rho_{ij})$ and $J_k^J = J_k(t, t+u_i + \rho_{ij} + u_j)$. Each of these terms can be evaluated using Lemmas 2 and 3. These results together with (39) give the objective function $\bar{J}_i(t, t+w)$ required for **RHCP2** in the form $\bar{J}_i(u_i, u_j)$ (again with a slight abuse of notation) where

$$\bar{J}_i(u_i, u_j) = -\frac{A(u_i, u_j)}{A(u_i, u_j) + B(u_i, u_j)}, \quad (40)$$

where $A(u_i, u_j) \triangleq J_i^A + J_j^A$, $B(u_i, u_j) \triangleq J_i^J + J_j^J + \sum_{k \in \mathcal{N}_i \setminus \{j\}} J_k^J$. Specifically, $A(u_i, u_j)$ and $B(u_i, u_j)$ takes the following forms:

$$\begin{aligned} A(u_i, u_j) &= a_1 + a_2 \log(1 + a_3 e^{-\lambda_i u_i}) \\ &\quad + a_4 \log(1 + a_5 e^{2A_j u_i} + a_6 e^{-\lambda_j u_j} + a_7 e^{2A_j u_i - \lambda_j u_j}) \\ &\quad + a_8 u_i + a_9 u_j, \end{aligned} \quad (41)$$

$$\begin{aligned} B(u_i, u_j) &= b_1 + b_2 u_i + b_3 u_j + b_4 e^{2A_j u_i} + b_5 e^{2A_i u_j} \\ &\quad + \sum_{k \in \mathcal{N}_i \setminus \{j\}} b_{6k} e^{2A_k(u_i + u_j)} + C(u_i, u_j), \end{aligned} \quad (42)$$

$$C(u_i, u_j) = c_1 \left[\frac{1 + c_2 e^{-\lambda_i u_i} + c_3 e^{2A_i u_j} + c_4 e^{-\lambda_i u_i + 2A_i u_j}}{1 + c_5 e^{-\lambda_i u_i}} \right],$$

where the coefficients $a_l, b_l, c_l, \forall l$ present in (41) and (42) are given in appendix A.

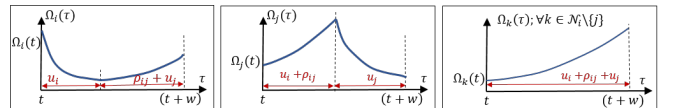


Fig. 4: State trajectories during $[t, t+w]$ for **RHCP1**.

c) **Unimodality of $\bar{J}_i(u_i, u_j)$** : Proving the unimodality of $\bar{J}_i(u_i, u_j)$ is a challenging task due to the complexity of the involved $A(u_i, u_j)$ and $B(u_i, u_j)$ expressions in (40). However, we establish that $\bar{J}_i(u_i, u_j)$ is unimodal along the lines $u_i = 0$ and $u_j = 0$. Further, we show that $\bar{J}_i(u_i, u_j) \rightarrow 0$ whenever $(u_i, u_j) \rightarrow (0, 0)$, $u_i \rightarrow \infty$ or $u_j \rightarrow \infty$. Based on these theoretical observations and the experimental results (see Fig. 5), we conjecture that $\bar{J}_i(u_i, u_j)$ is unimodal. However, to date, we have not provided a formal proof of this.

First, we slightly modify the Assumption 1 (to exclude the target i from the considered neighborhood $\mathcal{N}_i \setminus \{j\}$) as:

Assumption 2: $\sum_{k \in \mathcal{N}_i \setminus \{j\}} (2\Omega_k(t)A_k + Q_k) > 0$.

Again, we emphasize that this assumption holds whenever all the target dynamics are unstable [7]: $A_k \geq 0, \forall k$.

Lemma 5: The **RHCP1** objective function $\bar{J}_i(u_i, u_j)$ satisfies the following limits:

$$\begin{aligned} \lim_{(u_i, u_j) \rightarrow (0, 0)} \bar{J}_i(u_i, u_j) &= 0, \\ \lim_{u_i \rightarrow \infty} \bar{J}_i(u_i, 0) &= \begin{cases} L_i & \text{if } A_k < 0, \forall k \in \mathcal{N}_i \setminus \{j\}, \\ 0 & \text{otherwise,} \end{cases} \\ \lim_{u_j \rightarrow \infty} \bar{J}_i(0, u_j) &= \begin{cases} L_j & \text{if } A_k < 0, \forall k \in \mathcal{N}_i \setminus \{j\}, \\ 0 & \text{otherwise,} \end{cases} \\ \lim_{(u_i, u_j) \rightarrow (\infty, \infty)} \bar{J}_i(u_i, u_j) &= 0. \end{aligned} \quad (43)$$

where $L_i = -1/(1 + \frac{b_2}{a_8})$ and $L_j = -1/(1 + \frac{b_3}{a_9})$ (the coefficients b_2, a_8, b_3, a_9 are defined in Appendix A).

Proof: The result in (43) can be obtained by following the same steps used in the proof of Lemma 4. ■

Theorem 2: Under Assumption 2, the functions $\bar{J}_i(u_i, 0)$ and $\bar{J}_i(0, u_j)$ are unimodal.

Proof: This proof basically follows the same steps as the proof of Theorem 1. As an example, let us consider proving the unimodality of $\bar{J}_i(u_i, 0)$. First, $\bar{J}_i(u_i, 0)$ is written as $\bar{J}_i(u_i, 0) = -\bar{A}(u_i)/(\bar{A}(u_i) + \bar{B}(u_i))$ where $\bar{A}(u_i) = A(u_i, 0)$ and $\bar{B}(u_i) = B(u_i, 0)$. Therefore, similar to before, the nature of the stationary points of $\bar{J}_i(u_i, 0)$ is dependent on the sign of $\bar{A}\bar{B}'' - \bar{B}\bar{A}''$. Next, using $A(u_i, u_j)$ and $B(u_i, u_j)$ expressions in (41) and (42), we can write

$$\begin{aligned} \bar{B}'' &= \frac{d^2 B(u_i, 0)}{du_i^2} = 4A_j^2 b_4 e^{2A_j u_i} + \sum_{k \in \mathcal{N}_i \setminus \{j\}} 4A_k^2 b_{6k} e^{2A_k u_i} \\ &\quad + \frac{c_1 c_5 (1 + c_3) \lambda_i^2 e^{-\lambda_i u_i} (-1 + c_5 e^{-\lambda_i u_i})}{(1 + c_5 e^{-\lambda_i u_i})^3}, \\ \bar{A}'' &= \frac{d^2 A(u_i, 0)}{du_i^2} = \frac{\lambda_i^2 a_2 a_3 e^{-\lambda_i u_i}}{(1 + a_3 e^{-\lambda_i u_i})^2}. \end{aligned}$$

Finally, using the above two expressions and the coefficients shown in Appendix A, it can be proven that if $\Omega_i(t) > \Omega_{i,ss}$, for all $u_i \geq 0$, $\bar{B}'' > 0$ and $\bar{A}'' < 0$. Since $\bar{A}, \bar{B} > 0, \forall u_i \geq 0$, we can conclude that $\bar{A}\bar{B}'' - \bar{B}\bar{A}'' > 0, \forall u_i \geq 0$.

This result, together with the limits established in Lemma 5 implies that there exists only one stationary point in $\bar{J}_i(u_i, 0)$, which is the global minimizer. Further, since $\bar{J}_i(u_i, 0)$ and all of its derivatives are continuous, it can also

be concluded that $\bar{J}_i(u_i, 0)$ is a unimodal function. Following the same steps, the unimodality of $\bar{J}_i(0, u_j)$ can also be established. ■

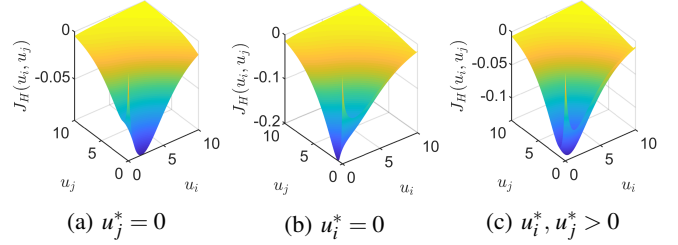


Fig. 5: Three example cases of **RHCP1** objective function $\bar{J}_i(u_i, u_j)$ plots (location of the minimizer: (u_i^*, u_j^*)).

d) **Solving RHCP1 for Optimal Controls u_i^*, u_j^*** : The solution u_i^*, u_j^* of (18) is given by

$$\begin{aligned} (u_i^*, u_j^*) &= \arg \min_{u_i, u_j} \bar{J}_i(u_i, u_j), \\ 0 &\leq u_i, \quad 0 \leq u_j, \\ u_i + u_j &\leq H - \rho_{ij} \end{aligned} \quad (44)$$

In (44), the feasible space is convex and we already conjectured that the objective function is unimodal. Therefore, again, we use the projected gradient descent algorithm to obtain the optimal control decisions (u_i^*, u_j^*) in (44).

e) **Solving for Optimal Next-Visit Target j^*** : Using the obtained (u_i^*, u_j^*) values in (44) for all $j \in \mathcal{N}_i(t)$, we are now aware of the optimal trajectory costs $\bar{J}_i(u_i^*, u_j^*)$ for all $j \in \mathcal{N}_i(t)$. Based on (19), the optimal neighbor to plan as the next-visit target is given by

$$j^* = \arg \min_{j \in \mathcal{N}_i(t)} \bar{J}_i(u_i^*, u_j^*). \quad (45)$$

Upon solving **RHCP1**, the agent remains stationary (active) on target i for a duration of u_i^* or until any other event occurs. If the agent completes the determined active time u_i^* (i.e., if the corresponding event $[h \rightarrow u_i^*]$ occurs), the agent will have to subsequently solve an instance of **RHCP2** to determine the next-visit target and depart from target i . However, if a different event occurred before the anticipated event $[h \rightarrow u_i^*]$, the agent will have to re-solve **RHCP1** to re-compute the remaining active time at target i .

VI. APPLICATION OF MACHINE LEARNING

Recall that in order to solve a RHCP, an agent $a \in \mathcal{A}$ (residing in a target $i \in \mathcal{V}$ at an event time t) needs to solve the optimization problems (18) and (19). The problem in (18) involves solving $|\mathcal{N}_i|$ different optimization problems (one for each neighbor $j \in \mathcal{N}_i$) to get the optimal continuous controls $\{U_{ij}^* : j \in \mathcal{N}_i\}$. The subsequent problem in (19) is only a simple numerical comparison that determines the optimal next-visit target $j^* \in \mathcal{N}_i$. Upon solving this RHCP, the agent will only use $U_{ij^*}^*$ and j^* to make its immediate decisions. Therefore, the continuous controls: $\{U_{ij}^* : j \in \mathcal{N}_i \setminus \{j^*\}\}$ found when solving (18) are wastefully discarded.

Intuitively, if j^* can be determined ahead of solving (18), we can prevent the aforementioned waste in computational resources by limiting the evaluation of (18) only for the pre-determined neighbor j^* - to directly get $U_{ij^*}^*$. Roughly speaking, this approach should save $\frac{|\mathcal{N}_i^j|-1}{|\mathcal{N}_i^j|}$ fraction of the processing (CPU) time required to solve the RHCP (i.e., (18) and (19)).

a) Ideal Classification Function: The aim here is to approximate an ideal classification function $F_i : \mathbb{R}_{\geq 0}^{|\mathcal{N}_i^j|} \rightarrow \mathcal{N}_i$ of the form

$$j^* = F_i(X_i(t)), \quad (46)$$

where $X_i(t) = \{\Omega_j(t) : j \in \mathcal{N}_i^j\}$ is the local state at target i at time t and (based on the forms of (18) and (19))

$$F_i(X_i(t)) \triangleq \arg \min_{j \in \mathcal{N}_i} J_H(X_i(t), \arg \min_{U_{ij} \in \mathbb{U}} J_H(X_i(t), U_{ij}; H); H). \quad (47)$$

In the *machine learning* literature, this kind of an ideal classification function $F_i(X_i)$ is commonly known as an *underlying function* (or a *target function*) and X_i is considered as a *feature vector* [23].

We highlight that F_i is strictly dependent on: (i) the current target $i \in \mathcal{V}$, (ii) the agent $a \in \mathcal{A}$ and (iii) the RHCP type $l \in \{1, 2\}$. Therefore, F_i in actuality should be written as $F_i^{a,l}$ even though we omitted doing so for notational simplicity.

b) Classifier Function: Due to the complexity of this ideal classification function $F_i(X_i)$ in (47), we cannot analytically simplify it to obtain a closed form solution for a generic input (feature) X_i . Therefore, we use machine learning techniques to model $F_i(X_i)$ by an estimate of it - which we denote as $f_i(X_i; \mathcal{D}_i)$. Here, \mathcal{D}_i represents a collected *data-set* of size L and the notation $f_i(X_i; \mathcal{D}_i)$ implies that this *classifier function* has been constructed based on that data-set \mathcal{D}_i .

Since our aim is to develop a fully on-line persistent monitoring solution, the agent a itself has to collect this data-set \mathcal{D}_i based on its very first L instants where a **RHCP** of type l was fully solved at target i . Specifically, \mathcal{D}_i can be thought of as a set of input-output pairs: $\mathcal{D}_i = \{(X_i(\tau), j^*(\tau)) : \tau \in \Gamma_i^{a,l}\}$ where $\Gamma_i^{a,l}$ is the set of first L event times where the agent a fully solved a **RHCP** of type l at target i . Notice that similar to F_i , both f_i and the data-set \mathcal{D}_i are also dependent on the target i , agent a and the **RHCP** type l .

c) Application of Neural Networks: In order to construct the classifier function $f_i(X_i; \mathcal{D}_i)$, among many commonly used classification techniques such as linear classifiers, support vector machines, kernel estimation techniques, etc., we chose an *artificial neural networks* (ANN) based approach. This choice was made because of the key advantages that an ANN-based classification approach holds [23]: (i) generality, (ii) data-driven nature, (iii) non-linear modeling capability and (iv) the ability to provide posterior probabilities.

Let us denote a shallow feed forward ANN model as $y = h_i(x; \Theta)$ where x is the $|\mathcal{N}_i^j|$ -dimensional input feature vector and y (or $h_i(x; \Theta)$) is the $|\mathcal{N}_i^j|$ -dimensional output vector under the ANN weight parameters Θ . For simplicity, we

propose to use only one hidden layer with ten neurons with hyperbolic tangent sigmoid (*tansig*) activation functions. At the output layer, we propose to use the *softmax* activation function so that each component of the output (denoted as $\{(h_i(x; \Theta))_k : k \in \mathcal{N}_i^j\}$) will be in the interval $(0, 1)$.

Based on this ANN model, the classifier function is given by:

$$\hat{j}^* = f_i(X_i; \mathcal{D}_i) = \arg \max_{k \in \mathcal{N}_i} (h_i(X_i; \Theta^*))_k, \quad (48)$$

where Θ^* represents the optimal set of ANN weights obtained by training the ANN model $y = h_i(x; \Theta)$ on the data-set \mathcal{D}_i . Specifically, these optimal weights Θ^* are determined through back-propagation (and gradient descent) [23] such that the (standard) cross-entropy based cost function $H(\Theta)$ evaluated over the data-set $\mathcal{D}_i = \{(X_i(\tau), j^*(\tau)) : \tau \in \Gamma_i^{a,l}\}$ given by

$$H(\Theta) = \frac{1}{L} \left[\sum_{\tau \in \Gamma_i^{a,l}} \sum_{k \in \mathcal{N}_i} \mathbf{1}\{j^*(\tau) = k\} \log (h_i(X_i(\tau); \Theta))_k + \mathbf{1}\{j^*(\tau) \neq k\} \log (1 - (h_i(X_i(\tau); \Theta))_k) \right] + \frac{\lambda}{2L} \|\Theta\|^2, \quad (49)$$

is minimized (λ represents the regularization constant).

d) RHC with Learning (RHC-L): Needless to say, the optimal weights Θ^* (and hence the classifier function $f_i(X_i; \mathcal{D}_i)$ in (48)) are determined only when the agent a has accumulated a data-set \mathcal{D}_i of length L . In other words, the agent a has to be familiar enough with solving the RHCP type l at target i in order to learn $f_i(X_i; \mathcal{D}_i)$.

Upon learning $f_i(X_i; \mathcal{D}_i)$, the RHCP given in (18) and (19) can be solved much efficiently by simply evaluating:

$$\hat{j}^* = f_i(X_i(t); \mathcal{D}_i), \quad (50)$$

$$U_{i\hat{j}^*}^* = \arg \min_{U_{ij^*} \in \mathbb{U}} J_H(X_i(t), U_{i\hat{j}^*}; H), \quad (51)$$

to directly obtain the optimal controls $U_i^*(t) = \{U_{i\hat{j}^*}^*, \hat{j}^*\}$. We label this approach as the RHC-L method.

Notice that (51) (when compared to (18)) only involves a single continuous optimization problem - which even maybe a redundant one to solve if the underlying RHCP is of type 2, where knowing the next target to visit (i.e., j^* now approximated by \hat{j}^*) is sufficient to take the immediate action. Therefore, the RHC-L method can be expected to have significantly lower processing times for evaluating the RHCPs faced by the agents (after the learning phase completes) compared to the RHC method.

The only drawback in this RHC-L approach when compared to the original RHC method is the performance degradation that can be expected due to learning related errors, i.e., due to the mismatch between $F_i(X_i)(= j^*)$ in (47) and its estimate $f_i(X_i; \mathcal{D}_i)(= \hat{j}^*)$ learned in (48).

e) RHC with Active Learning (RHC-AL): We next propose a technique to suppress the aforementioned performance degradation that stems from the learning related errors. For this purpose, we exploit the fact that ANN outputs

are actually estimates of the posterior probabilities [23]. This simply means

$$(h_i(X_i; \Theta^*))_k \simeq P(j^* = k|X_i), \quad (52)$$

where, $(h_i(X_i; \Theta^*))_k$ is the output of the ANN related to the neighbor $k \in \mathcal{N}_i$ and $P(j^* = k|X_i)$ is the probability of the ideal classification function $j^* = F_i(X_i)$ in (47) resulting $F_i(X_i) = k \in \mathcal{N}_i$, given the feature vector X_i . Note that $F_i(\cdot)$ here is an unknown function that we try to estimate and hence $j^* (= F_i(X_i))$ is a random variable.

Based on (52) and (48), the mismatch error between $F_i(X_i)$ and $f_i(X_i; \mathcal{D}_i)$ given the feature vector X_i can be estimated as $e_i(X_i)$ where

$$e_i(X_i) \triangleq P(F_i(X_i) \neq f_i(X_i; \mathcal{D}_i)|X_i) = 1 - \max_{k \in \mathcal{N}_i} (h_i(X_i; \Theta^*))_k. \quad (53)$$

Clearly, prior to solving the RHC-L problems (50) and (51), the agent can evaluate this mismatch error metric $e_i(X_i)$ and if it falls above a certain threshold (say 0.1), it can resort to follow the original RHC approach and solve (18) and (19), instead. Moreover, in such a case, the obtained RHC solutions can be incorporated into the data-set \mathcal{D}_i and re-train the ANN (to get a new Θ^* for $h_i(X_i; \Theta^*)$ in (48)).

We call this “active learning” approach as the RHC-AL method. It is essential to highlight that the RHC-AL approach helps agents to make correct decisions in the face of unfamiliar scenarios. Therefore, we can expect the RHC-AL method to perform well compared to the RHC-L method - only at the expense of trading off the advantage that the RHC-L method had in terms of the processing times compared to the RHC method.

Remark 1: The proposed on-line learning process can even be carried out off-line (if the system allows it) as each agent (for each target $i \in \mathcal{V}$ and each RHCP type) can synthetically generate data-sets \mathcal{D}_i exploiting the relationship (47) with a set of randomly generated features X_i . Moreover, if the agents are homogeneous, the proposed distributed learning process can be made centralized by allowing agents to share their data sets (pertaining to the same targets). However, the effectiveness of such a “shared data based learning” scenario is debatable as the optimal trajectory of each agent might be unique even though the agents are homogeneous characteristically.

VII. SIMULATION RESULTS

This section contains the details of three different simulation studies. In the first, we explore how the RHC based agent control method performs compared to four other agent control techniques, in terms of the performance metric J_T defined in (7) evaluated over a relatively short period: $T = 50.s$. Second, we study how effective a target state control strategy can be under the target state estimates provided by different agent control methods. Finally, we explore the long term performance of agent controllers by selecting $T = 750.s$. In particular, we compare the agent control methods: RHC, RHC-L and RHC-AL in terms of the performance metric J_T

and the average processing (CPU) time taken to solve each RHCP.

Persistent Monitoring Problem Configurations: We consider the four randomly generated persistent monitoring problem configurations (PCs) shown in Fig. 6. Blue circles represents the targets and dark black lines indicate the trajectory segments that are available for the agents to travel between targets. Agents and target error covariance values at $t = 0$ are represented by red triangles and yellow vertical bars/blue texts respectively (see Fig. 8 for PCs at $t = T$). The PCs 1,2 has seven targets and two agents each and the PCs 3,4 has ten targets and four agents each. In each PC, the target parameters were selected using the uniform distribution $U[\cdot, \cdot]$ as follows: $Y_i \sim U[0, 1]$, $A_i \sim U[0.01, 0.41]$, $B_i \sim U[0.01, 0.41]$, $Q_i \sim U[0.1, 2.1]$, $R_i \sim U[2, 10]$ and we set $H_i = 1, \forall i \in \mathcal{V}$. If the distance between any two targets is less than a certain threshold σ , we deploy a linear shaped trajectory segment between those targets. For the PC 1, $\sigma = 0.7$ (dense) was used and for the reset, $\sigma = 0.45$ (sparse) was used. Each agent is assumed to travel with a unit speed on these trajectory segments.

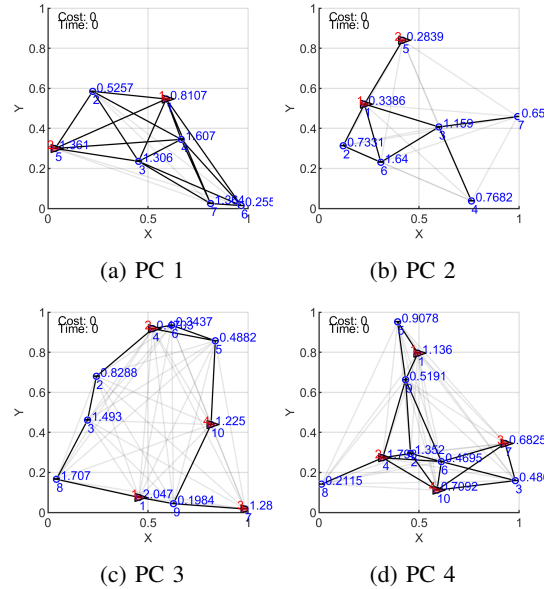


Fig. 6: Used four randomly generated persistent monitoring problem configurations (PCs) and their initial conditions.

A. Simulation Study 1: The effect of agent controls on target state estimation over a relatively short period.

In this section, we compare the performance metric J_T (defined in (7) with $T = 50$) observed for the four PCs shown in Fig. 6 when using five different agent control methods: (i) the centralized and off-line periodic control (MTSP) method proposed in [7] (ii) a basic distributed and on-line control (BDC) method, (iii) the proposed RHC method, (iv) a periodic version of the BDC (BDC-P) method and (v) a periodic version of the RHC (RHC-P) method. In fact, this simulation study is aimed to observe the effectiveness of

the overall *target state estimation* process (as it is directly reflected by the metric J_T) rendered by the aforementioned different agent controllers. According to (4), the choice of target controls $v_i(t)$ in (1) do not affect J_T . Hence in this study, we set: $v_i(t) = 0, \forall i \in \mathcal{V}, \forall t \in [0, T]$.

a) **The Basic Distributed Control (BDC) Method:** The BDC method uses the same event-driven control architecture. However, the difference (w.r.t. the RHC method) lies in the used u_i^* and j^* choices in (18) and (19). In particular, the BDC method uses:

$$\begin{aligned} u_i^* &= \arg \min_{\tau \geq 0} \mathbf{1}\{\Omega_i(t + \tau) \leq (1 + \varepsilon)\Omega_{i,ss}\}, \\ j^* &= \arg \max_{j \in \mathcal{N}_i(t)} \Omega_j(t) \end{aligned} \quad (54)$$

with $\varepsilon = 0.075$ and $\Omega_{i,ss}$ (which represents the steady-state error covariance value of target i) in (32). In a nut shell, the BDC method forces an agent to dwell at each visited target i until its error covariance $\Omega_i(t)$ drops to an ε fraction closer to the corresponding target's $\Omega_{i,ss}$ value. Upon completing this requirement, the next-visit target is determined as the neighbor j in $\mathcal{N}_i(t)$ with the maximum $\Omega_j(t)$ value.

b) **The Centralized and Off-line Control (MTSP) Method [7]:** Unlike the distributed and on-line agent control methods: RHC and BDC, the MTSP method proposed in [7] fully computes the agent trajectories in a centralized off-line stage, focusing on minimizing an infinite horizon objective function of the form

$$\max_{i \in \mathcal{V}} \limsup_{t \rightarrow \infty} \text{tr}(\Omega_i(t)) \quad (55)$$

via selecting appropriate periodic agent trajectories. Nevertheless, this objective function is in the same spirit of J_T (7) as it also aims to maintain the target error covariances as low as possible.

The MTSP method first uses the spectral clustering algorithm [24] to decompose the target topology \mathcal{G} into sub-graphs among the agents. Then, on each sub-graph, starting from the *traveling salesman problem* (TSP) solution, a greedy target visitation cycle is constructed. Essentially, this set of target visitation cycles is a candidate solution for the famous multi-TSP [25] (hence the acronym for [7]: MTSP). Finally, the dwell-time spent at each target (on the constructed target visitation cycle) is found using a golden ratio search algorithm exploiting many interesting mathematical properties. In essence, the MTSP method constructs a periodic solution to a given PMN problem.

c) **Hybrid Methods: BDC-P and RHC-P:** In some applications, having a periodicity in visiting targets can be a crucial constraint (e.g., Bus routes). Even in such cases, the proposed RHC method (or the BDC method) can still be used to make the dwell-time decisions at each visited target instead of using a fixed set of predetermined dwell-times like in the MTSP method. The optimal next-visit target, i.e., j^* in (19) (or in (54)) would now be given by the off-line computed target visitation cycles (similar to the MTSP method). We use the label RHC-P (or BDC-P) to represent such a hybrid periodic agent control method. Note that in this

RHC-P method, when solving for the dwell-times, (i.e., (18)), the RHCP objective (22) should only consider neighboring targets in the agent's target visitation cycle. Pertaining to the PCs shown in Fig. (6), respective periodic target visitation cycles used by the periodic agent control methods (MTSP, BDC-P and RHC-P) are shown in Fig. 7.

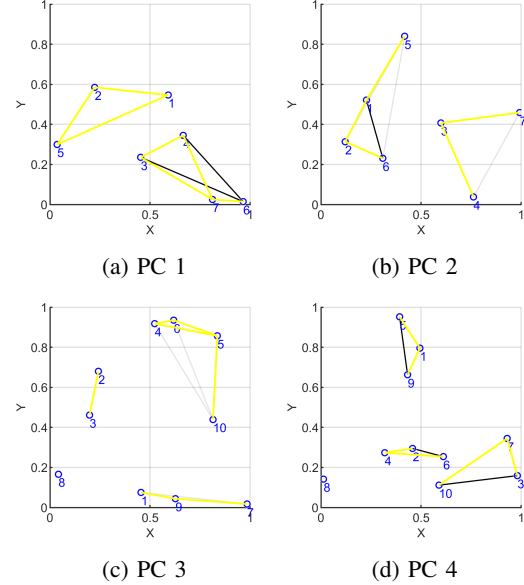


Fig. 7: Periodic agent trajectories (yellow colored contours) used by the methods: MTSP, BDC-P and RHC-P.

Results and Discussion: Obtained results from the comparison are summarized in Tab. I. According to those results, on average, the RHC method has outperformed all the other agent control methods. It can be seen that the RHC-P method has the second-best performance level, and it has even performed slightly better than the RHC method in two cases. This is justifiable because the RHC-P method has a significant centralized and off-line component compared to the RHC method, which is completely distributed and on-line. Corresponding final states of the PCs given by the RHC method are shown in Fig. 8.

TABLE I: Performance comparison of target state estimation (i.e., J_T) under five agent control methods in four PCs.

Target State Estimator Performance (J_T)	Agent Control Mechanism					
	Off-line	Off-line/On-line		On-line		
	MTSP	BDC-P	RHC-P	BDC	RHC	
PC No.	1	99.88	119.23	84.41	88.68	88.16
	2	90.08	155.25	77.80	101.75	70.51
	3	133.50	268.85	128.90	162.48	132.83
	4	187.88	231.28	123.70	174.32	113.30
Average:	127.83	193.65	103.70	131.81	101.20	

Worst Case Performance: Inspired by the objective function (55) [7], we define the *worst case performance* of an agent controller over the period $[0, T]$ as J_W where

$$J_W = \max_{i \in \mathcal{V}, t \in [0, T]} \text{tr}(\Omega_i(t)). \quad (56)$$

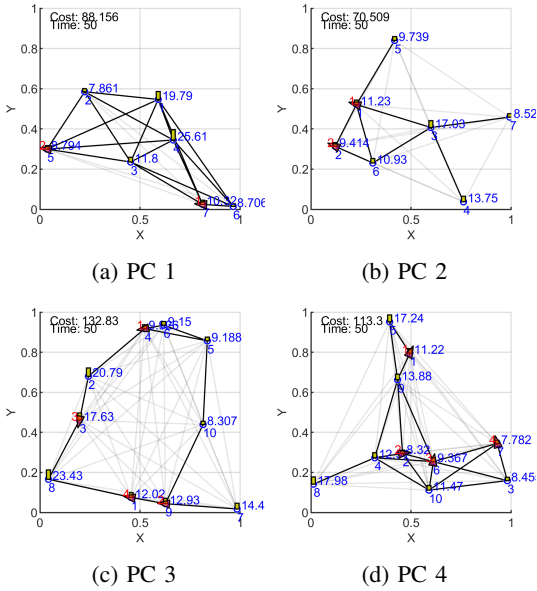


Fig. 8: Final state of the PCs after using the RHC method.

In our case, J_W is simply the maximum recorded target error covariance value in the target topology over the period $[0, T]$. For the same experiments that gave the results shown in Tab. I, we have evaluated the corresponding J_W (56) value. The obtained results are summarized in Tab. II. According to these experimental results, it is evident that the periodic agent control methods have an advantage compared to the fully distributed and on-line methods like RHC and BDC in terms of worst-case performance. Nevertheless, the fact that the RHC-P method has obtained the best average J_W value (and the second-best average J_T value) implies that the proposed RHC method can be effectively adopted for different problem settings (with different constraints, objectives, etc.).

TABLE II: Performance comparison of worst case target state estimation (i.e., J_W) under five agent control methods in four PCs.

The Worst Case Target State Estimator Performance (J_W)		Agent Control Mechanism				
		Off-line	Off-line/On-line		On-line	
		MTSP	BDC-P	RHC-P	BDC	RHC
PC No.	1	40.23	288.34	50.19	96.33	71.57
	2	38.03	586.19	65.62	270.42	32.29
	3	47.54	427.53	46.52	386.66	306.84
	4	115.74	403.38	49.26	487.65	77.41
Average:		60.38	426.36	52.90	310.27	122.03

B. Simulation Study 2: The effect of agent controls on target state controllers over a relatively short period

In this simulation study, we explore a byproduct of achieving reasonable target state estimates: the ability to control the target states effectively. Here, we assume each target has its own tracking control task that needs to be achieved through a simple local state feedback control mechanism. Clearly, for this purpose, each target has to rely on its state estimate - of which the accuracy deteriorates when the target is not visited by an agent regularly. We define a new metric: J_C to

represent the performance of the overall *target state control* process and compare the obtained J_C values by different agent controllers under different PCs.

a) **Target Control Mechanism:** In this section, we assume each target $i \in \mathcal{V}$ has to control its state $\phi_i(t)$ such that a signal

$$y_i(t) = C_i \phi_i(t) + D_i, \quad (57)$$

tracks a given reference signal $r_i(t)$ (C_i, D_i are also given).

Let us define the tracking error as $e_i(t) = y_i(t) - r_i(t)$. In order to make $e_i(t)$ follow the (asymptotically stable) dynamics: $\dot{e}_i = -K_i e_i(t)$, the target i needs to select its control input $u_i(t)$ in (1) as (also recall (11))

$$u_i(t) = -\frac{1}{B_i C_i} (C_i(A_i + K_i)\phi_i(t) + K_i D_i - (\dot{r}_i(t) + K_i r_i(t))). \quad (58)$$

However, since target i is unaware of its state ϕ_i , naturally, it can use the state estimate $\hat{\phi}_i$ in (3) in the state feedback control law as

$$u_i(t) = -\frac{1}{B_i C_i} (C_i(A_i + K_i)\hat{\phi}_i(t) + K_i D_i - (\dot{r}_i(t) + K_i r_i(t))). \quad (59)$$

To measure the performance of this tracking control task, we propose to use the performance metric J_C where

$$J_C \triangleq \frac{1}{T} \int_0^T |e_i(t)| dt. \quad (60)$$

b) **Results and Discussion:** In this study, we set $C_i = 1$, $D_i = 0$, $K_i = 2$ and select the reference signal that needs to be tracked as: $r_i(t) = 10 \sin(2t + i)$, $\forall i \in \mathcal{V}$. The metric J_C observed for different PCs with different agent controllers are summarized in Tab III. Similar to before, obtained results show that the RHC method, on average, has outperformed all the other agent controllers. Corresponding final states of the PCs observed under the RHC method are shown in Fig. 9. The red vertical bars (on top of yellow vertical bars) represent the absolute tracking error $|e_i(t)|$ of each target i at $t = T$. These results imply that having an agent control mechanism that provides superior target state estimation capabilities (i.e., lower J_T) enables the targets to have better control over their states (i.e., lower J_C).

TABLE III: Performance comparison of target state controllers (i.e., J_C) under five agent control methods in four PCs.

Target State Controller Performance ($J_C \times T$)		Agent Control Mechanism				
		Off-line	Off-line/on-line		On-line	
		MTSP	BDC-P	RHC-P	BDC	RHC
PC No.	1	57.97	51.99	50.99	48.40	48.12
	2	51.66	56.80	52.35	55.54	50.14
	3	73.81	81.40	74.08	80.89	74.33
	4	85.76	86.34	77.35	86.61	75.81
Average:		67.30	69.13	63.69	67.86	62.10

C. Simulation Study 3: Long term performance with learning

In both previous simulation studies, we focused on a relatively short period ($T = 50s$) that essentially encompassed the transient phase of the system (which, in general,

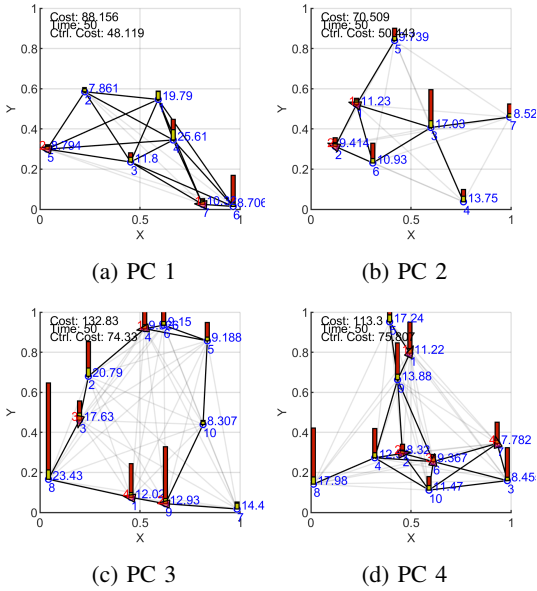


Fig. 9: Final state of the PCs after using the RHC method with target state control.

is the most challenging part to control/regulate). However, in this final simulation study, we aim to explore the agent controllers' performance over a lengthy period ($T = 750$ s) so that it includes both the transient and the steady-state phases of the system. Note that this kind of a problem setting is ideal for deploying the machine learning based RHC solutions: RHC-L and RHC-AL proposed in Section VI of this paper. Therefore, in this study, we specifically compare the three controllers: RHC, RHC-L and RHC-AL for the PCs 1 and 2, in terms of the evolution of: (i) the performance metric J_t (7) and (ii) the average processing time (also called the "CPU time") taken to solve a RHCP, throughout the simulation time $t \in [0, T]$. These CPU times were recorded on an Intel Core i7-8700 CPU 3.20 GHz Processor with a 32 GB RAM.

As shown in Figs. 10(a) and 11(a), the RHC method takes the highest amount of CPU time to solve a RHCP. Its upward trend in the initial stages of the simulations indicates a transient phase of the processor. We highlight that this transient phase is independent of that of J_t curves shown in Figs. 10(b) and 11(b). Table IV shows that based on the steady-state averages for the PC 1 (Fig. 10), the RHC-L method spends 86.5% less CPU time compared to the RHC method but at a loss of 4.7% in performance. For the same PC, the RHC-AL method shows a 66.7% reduction in CPU time while having only a 0.1% loss in performance.

In these simulations of RHC-L and RHC-AL methods, for the on-line training of classifiers $f_i(X_i; \mathcal{D}_i)$ (required in (50)), we have set the data-set size to be 25 (i.e., $|\mathcal{D}_i| = 25$). As implied by Figs 10(a) and 11(a), agents have been able to collect that amount of data points well within their transient phase (of the J_t curve). Even though learning based on transient data has a few advantages, it is mostly regarded as ineffective - especially if the learned controller would

TABLE IV: Average over the steady-state period $t \in [500, 750]$ of the curves in Figs. 10 and 11.

Average over steady-state: (Interval: [500, 750])		RHC	RHC-L	RHC-LE	RHC-AL
PC 1	CPU Time	10.589	1.4287	2.3787	3.5259
	J_t	96.1315	100.6107	96.1315	96.2686
PC 2	CPU Time	3.7909	0.9666	1.1808	1.7334
	J_t	80.2887	82.1902	80.2893	83.9678

mostly operate in a steady-state condition. Therefore, we next extend the data-set size to be $|\mathcal{D}_i| = 75$ and execute the same RHC-L method, which henceforth is labeled as the RHC-LE method. According to the summarized steady-state averaged data given in Tab IV, for the PC 1 and 2, the RHC-LE method respectively shows 77.5% and 68.9% reductions in CPU time compared to the RHC method - while having almost no losses in performance ($< 0.001\%$) in both cases.

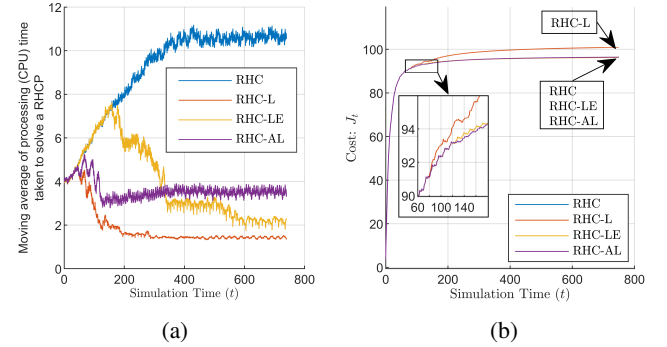


Fig. 10: Evolution of the average processing time taken to solve a RHCP and the objective function value for PC 1.

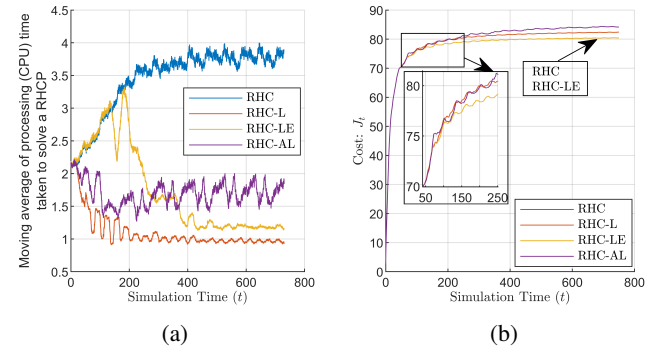


Fig. 11: Evolution of the average processing time taken to solve a RHCP and the objective function value for PC 2.

VIII. CONCLUSION

The aim of the multi-agent persistent monitoring problem in this paper is to observe the target states and minimize an overall measure of error covariance evaluated over a finite period. Compared to existing centralized and off-line control solutions, a novel computationally efficient distributed and on-line solution is proposed based on event-driven receding horizon control. In particular, each agent determines their

optimal planning horizon and the immediate sequence of optimal decisions at each event of interest faced in its trajectory. Numerical results show higher performance levels compared to existing other both centralized and distributed agent control methods. Future work will aim to generalize the proposed solution for multidimensional target state dynamics and combine distributed estimation with target state control.

APPENDIX

A. Coefficients of the *RHCPI* objective function (40)

$$\begin{aligned}
a_1 &= \frac{1}{G_j} \log \left[\frac{G_j - 2A_j v_{j1}}{2A_j(v_{j2} - v_{j1})} \right] + \frac{1}{G_i} \log \left[\frac{-G_i \Omega_i - Q_i}{Q_i(v_{i2} - v_{i1})} \right], \\
a_2 &= \frac{1}{G_i}, \quad a_3 = -\frac{G_i \Omega_i + Q_i v_{i2}}{G_i \Omega_i + Q_i v_{i1}}, \quad a_4 = \frac{1}{G_j}, \\
a_5 &= -\frac{v_{j2}(2A_j \Omega_j + Q_j) e^{2A_j \rho_{ij}}}{Q_j v_{j2} + 2A_j}, \quad a_6 = -\frac{G_j - 2A_j v_{j2}}{G_j - 2A_j v_{j1}}, \\
a_7 &= -a_5, \quad a_8 = \frac{1}{v_{i1}}, \quad a_9 = \frac{1}{v_{i2}}, \\
b_1 &= -\frac{Q_i}{4A_i^2} (1 + 2A_i \rho_{ij}) - \frac{Q_j}{4A_j^2} (1 + 2A_j \rho_{ij}) - \frac{\Omega_j}{2A_j} \\
&\quad - \sum_{k \in \mathcal{N}_i \setminus \{j\}} \left[\frac{Q_k}{4A_k^2} (1 + 2A_k \rho_{ij}) + \frac{\Omega_k}{2A_k} \right], \\
b_2 &= -\sum_{k \in \mathcal{N}_i} \frac{Q_k}{2A_k}, \quad b_3 = -\sum_{k \in \mathcal{N}_i \setminus \{j\}} \frac{Q_k}{2A_k}, \\
b_4 &= \frac{1}{4A_j^2} (Q_j + 2A_j \Omega_j) e^{2A_j \rho_{ij}}, \quad b_5 = \frac{Q_i}{4A_i^2} e^{2A_i \rho_{ij}}, \\
b_{6k} &= \frac{1}{4A_k^2} (Q_k + 2A_k \Omega_k) e^{2A_k \rho_{ij}}, \\
c_1 &= -\frac{1}{2A_i v_{i1}}, \quad c_2 = -\frac{v_{i1} \Omega_i - 1}{v_{i2} \Omega_i - 1}, \quad c_3 = -e^{2A_i \rho_{ij}}, \\
c_4 &= -c_2, \quad c_5 = -\frac{G_i \Omega_i + Q_i v_{i2}}{G_i \Omega_i + Q_i v_{i1}}.
\end{aligned}$$

REFERENCES

- [1] K. Leahy, D. Zhou, C. I. Vasile, K. Oikonomopoulos, M. Schwager, and C. Belta, "Persistent Surveillance for Unmanned Aerial Vehicles Subject to Charging and Temporal Logic Constraints," *Autonomous Robots*, vol. 40, no. 8, pp. 1363–1378, 2016.
- [2] S. L. Smith, M. Schwager, and D. Rus, "Persistent Monitoring of Changing Environments Using a Robot with Limited Range Sensing," in *Proc. of IEEE Intl. Conf. on Robotics and Automation*, 2011, pp. 5448–5455.
- [3] J. Trevathan and R. Johnstone, "Smart Environmental Monitoring and Assessment Technologies (SEMAT) A New Paradigm for Low-Cost, Remote Aquatic Environmental Monitoring," *Sensors (Switzerland)*, vol. 18, no. 7, 2018.
- [4] N. Mathew, S. L. Smith, and S. L. Waslander, "Multirobot Rendezvous Planning for Recharging in Persistent Tasks," *IEEE Trans. on Robotics*, vol. 31, no. 1, pp. 128–142, 2015.
- [5] N. Zhou, C. G. Cassandras, X. Yu, and S. B. Andersson, "Optimal Threshold-Based Distributed Control Policies for Persistent Monitoring on Graphs," in *Proc. of American Control Conf.*, 2019, pp. 2030–2035.
- [6] N. Rezazadeh and S. S. Kia, "A Sub-Modular Receding Horizon Approach to Persistent Monitoring for A Group of Mobile Agents Over an Urban Area," in *IFAC-PapersOnLine*, vol. 52, no. 20, 2019, pp. 217–222.
- [7] S. C. Pinto, S. B. Andersson, J. M. Hendrickx, and C. G. Cassandras, "Optimal Minimax Mobile Sensor Scheduling Over a Network," 2020. [Online]. Available: <https://arxiv.org/abs/2009.11386>
- [8] J. Yu, S. Karaman, and D. Rus, "Persistent Monitoring of Events With Stochastic Arrivals at Multiple Stations," *IEEE Trans. on Robotics*, vol. 31, no. 3, pp. 521–535, 2015.
- [9] S. Welikala and C. G. Cassandras, "Asymptotic Analysis for Greedy Initialization of Threshold-Based Distributed Optimization of Persistent Monitoring on Graphs," in *Proc. of 21st IFAC World Congress*, 2020.
- [10] S. K. Hari, S. Rathinam, S. Darbha, K. Kalyanam, S. G. Manyam, and D. Casbeer, "The Generalized Persistent Monitoring Problem," in *Proc. of American Control Conf.*, vol. 2019-July, 2019, pp. 2783–2788.
- [11] S. Welikala and C. G. Cassandras, "Event-Driven Receding Horizon Control For Distributed Persistent Monitoring on Graphs," in *Proc. of 59th IEEE Conf. on Decision and Control (to appear)*, 2020.
- [12] Y.-W. Wang, Y.-W. Wei, X.-K. Liu, N. Zhou, and C. G. Cassandras, "Optimal Persistent Monitoring Using Second-Order Agents with Physical Constraints," *IEEE Trans. on Automatic Control*, vol. 64, no. 8, pp. 3239–3252, 2017.
- [13] P. Maini, K. Yu, P. B. Sujit, and P. Tokekar, "Persistent Monitoring with Refueling on a Terrain Using a Team of Aerial and Ground Robots," in *Proc. of IEEE Intl. Conf. on Intelligent Robots and Systems*, 2018, pp. 8493–8498.
- [14] N. Zhou, X. Yu, S. B. Andersson, and C. G. Cassandras, "Optimal Event-Driven Multi-Agent Persistent Monitoring of a Finite Set of Data Sources," *IEEE Trans. on Automatic Control*, vol. 63, no. 12, pp. 4204–4217, 2018.
- [15] C. Song, L. Liu, G. Feng, and S. Xu, "Optimal Control for Multi-Agent Persistent Monitoring," *Automatica*, vol. 50, no. 6, pp. 1663–1668, 2014.
- [16] W. Li and C. G. Cassandras, "A Cooperative Receding Horizon Controller for Multi-Vehicle Uncertain Environments," *IEEE Trans. on Automatic Control*, vol. 51, no. 2, pp. 242–257, 2006.
- [17] S. S. Park, Y. Min, J. S. Ha, D. H. Cho, and H. L. Choi, "A Distributed ADMM Approach to Non-Myopic Path Planning for Multi-Target Tracking," *IEEE Access*, vol. 7, pp. 163 589–163 603, 2019.
- [18] X. Lan and M. Schwager, "Planning Periodic Persistent Monitoring Trajectories for Sensing Robots in Gaussian Random Fields," in *Proc. of IEEE Intl. Conf. on Robotics and Automation*, 2013, pp. 2415–2420.
- [19] S. He, H. S. Shin, S. Xu, and A. Tsourdos, "Distributed Estimation Over a Low-Cost Sensor Network: A Review of State-Of-The-Art," *Information Fusion*, vol. 54, pp. 21–43, 2020.
- [20] Y. Khazaeni and C. G. Cassandras, "Event-Driven Cooperative Receding Horizon Control for Multi-Agent Systems in Uncertain Environments," *IEEE Trans. on Control of Network Systems*, vol. 5, no. 1, pp. 409–422, 2018.
- [21] R. Chen and C. G. Cassandras, "Optimization of Ride Sharing Systems Using Event-driven Receding Horizon Control," in *Proc. of 2020 Intl. Workshop on Discrete Event Systems (to appear)*, 2020.
- [22] L. Dieci and A. Papini, "Conditioning of the Exponential of a Block Triangular Matrix," *Numerical Algorithms*, vol. 28, no. 1-4, pp. 137–150, 2001.
- [23] G. P. Zhang, "Neural Networks for Classification: A Survey," *IEEE Trans. on Systems, Man and Cybernetics Part C: Applications and Reviews*, vol. 30, no. 4, pp. 451–462, 2000.
- [24] U. von Luxburg, "A Tutorial on Spectral Clustering," 2007. [Online]. Available: <http://arxiv.org/abs/0711.0189>
- [25] T. Bektas, "The Multiple Traveling Salesman Problem: An Overview of Formulations and Solution Procedures," *Omega*, vol. 34, no. 3, pp. 209–219, 2006.